Impurity and Lattice Scattering Parameters as Determined from Hall and Mobility Analysis in n-Type Silicon*

P. Norton,† T. Braggins, and H. Levinstein
Department of Physics, Syracuse University, Syracuse, New York 13210
(Received 4 June 1973)

The carrier concentration and mobility, as determined from the Hall effect, have been analyzed using a computer for a series of n-type silicon samples doped with Sb, P, and As. Mobility calculations, performed numerically, were based on the general treatment given by Herring and Vogt. Ionized-impurity scattering was calculated from two theories and compared with experiment. Lattice-scattering parameters for intervalley and accoustic modes were determined from a comparison of the results between theory and experiment, using as many as four intervalley phonons. The conclusions support the earlier work of Long, and a partial explanation of the disagreement with parameters determined from other measurements is suggested. Scattering by neutral impurities is found to be temperature dependent, unlike the theoretical model of Erginsoy.

I. INTRODUCTION

The Hall effect has been studied and analyzed in detail for a series of n-type silicon samples doped with antimony, phosphorus, and arsenic. Measurements were made on samples with doping densities ranging from 4×10^{13} to 8×10^{16} cm^{-3}, generally between 20 and 160 K, but over a wider temperature range in some cases. Almost all the data were taken in the high-magnetic-field limit so that Hall-factor corrections were not needed to determine the carrier concentration and drift mobility. We have analyzed both the carrier concentration and the mobility as a function of temperature. For the mobility analysis, the model of Herring and Vogt[1] was adopted to approximate the anisotropic nature of the conduction band. By using the results of both carrier-concentration and mobility analyses, we have been able to determine independently the density of compensating acceptors in these samples. Therefore, a quantitative comparison could be made between two models of ionized-impurity scattering, since this mechanism is coupled directly to the compensation density at low temperatures. In particular, we have compared the formulation of Brooks,[2] Herring, and Dingle[3] given for isotropic scattering, to the theory given by Samoilovich *et al.*,[4–6] calculated expressly for the case of spheriodal anisotropic bands.

Recent controversy over the intervalley lattice scattering process in silicon has been examined, and lattice scattering parameters have been fit to our data using a number of proposed models. Our two purest samples were used for this purpose. The results of this test are in good agreement with similar results of Long,[7] but do not support parameters determined from the analysis of photoconductivity and recombination-radiation experiments. In part, a reinterpretation of some optical experiments is suggested to clarify the present disagreement between optical and transport measurements.

We have found that neutral-impurity scattering is not well described by present theory. Experimental data for the mobility due to neutral-impurity scattering are shown to have a substantial temperature dependence, not accounted for by the Erginsoy[8] formulation of this problem. Part of this discrepancy is qualitatively resolved in terms of resonant scattering involving a possible bound state for the scattered electron as described by Sclar.[9] At higher temperatures, however, inelastic scattering may explain the temperature dependence. A much weaker neutral-impurity scattering interaction is apparent for arsenic-doped silicon than for antimony- or phosphorus-doped samples. No explanation could be found for this difference.

II. HALL-EFFECT MEASUREMENTS AND CARRIER-CONCENTRATION ANALYSIS

The experimental apparatus for measuring the Hall effect has been described previously.[10] In the case of silicon, bridge-type samples were contacted with welded gold wires containing 0.6-at.% Sb. Orientation of the magnetic field was in the ⟨111⟩ direction. The electric field was applied along the ⟨110⟩ or ⟨211⟩ axis.

Analysis of the Hall effect in silicon has been complicated by the Hall factor r which depends on the strength of the various scattering mechanisms, and the details of the band structure.[11] Long and Myers[12] used an iterative procedure to calculate the Hall factor in their analysis of carrier concentration and mobility as a function of temperature. In the limit of high magnetic fields, the Hall factor becomes unity and can be ignored. Since very little data have been published on the variation of the Hall coefficient with magnetic field, we ran a

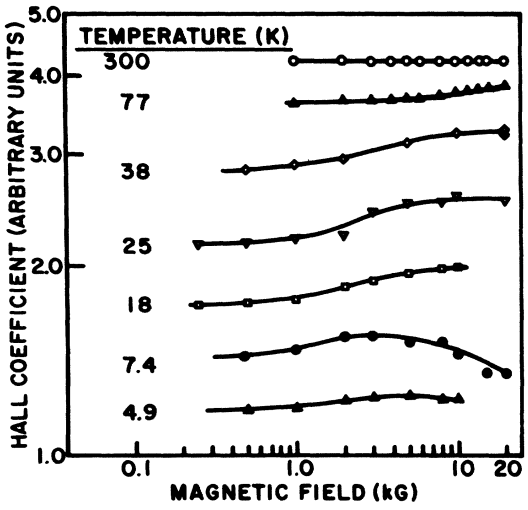

FIG. 1. Hall coefficient (arbitrary units) as a function of magnetic field, as measured for Si: As 1 (see Table I). The decrease in the Hall coefficient at high fields at the lowest temperatures is probably fictitious, due to the field dependence of the carrier lifetime.

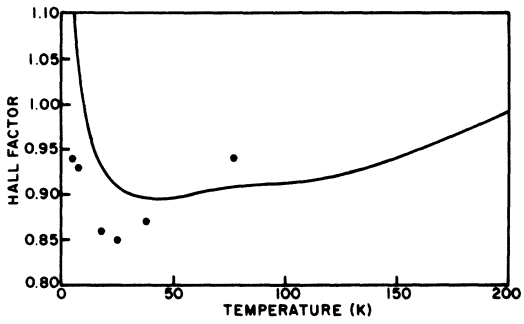

FIG. 2. Ratio of low-field to high-field Hall coefficient, as shown in Fig. 1 for Si: As 1, compared to the calculated Hall factor r. The Hall factor is calculated from Eq. (1), using the parameters determined for this sample listed in Table VI and mobility parameters for lattice scattering listed in Table IV.

series of magnetic field sweeps on an arsenic-doped lightly compensated sample. Figure 1 shows the Hall coefficient as a function of magnetic field strength for a number of temperatures in the range 5–300 K. The data below about 20 K were obtained by magnetic field sweeps of the photo-Hall coefficient. 300-K background illumination, filtered by cold InSb, restricted the radiation to $\lambda > 5\ \mu$m. The slight decrease in the photo-Hall coefficient at the highest magnetic fields, as seen in Fig. 1, is probably due to the Hall voltage approaching the region where carrier lifetime becomes dependent on the electric field. The ratio of the low- to high-field coefficient is shown in Fig. 2 as a function of temperature. For comparison, we have calculated the Hall factor r using the expression given by Herring and Vogt, [1] and in agreement with Long[7]:

$$r = \frac{3(\langle\tau_\perp^2\rangle/m_\perp^{*2} + 2\langle\tau_\perp\tau_\parallel\rangle/m_\perp^* m_\parallel^*)}{[2(\langle\tau_\perp\rangle/m_\perp^*) + \langle\tau_\parallel\rangle/m_\parallel^*]^2}, \qquad (1)$$

where $\perp$, $\parallel$ refer to the transverse and longitudinal directions of the ellipsoidal bands and τ and m^* are the relaxation times and masses of the electrons. These will be fully explained in Sec. III. It should be mentioned that a somewhat less exact expression was used for calculating r by Long and Myers, since isotropic scattering was assumed. [13] As can be seen, there is fair agreement between the values deduced from the field sweep data and those calculated from Eq. (1). Disagreement at the lowest temperatures may be due, in part, to a failure of the Born approximation used to calculate ionized-impurity scattering in this region, and also from the lack of an adequate theory to correctly describe neutral-impurity scattering which was quite strong in this sample. For our purposes, we have used data taken from the high-field limit and set the Hall factor equal to unity. This approximation is good for temperatures below about 100 K, depending on the strength of impurity scattering. We have used data up to about 160 K in some cases without correction. This should introduce very little error, even though the high-field limit cannot quite be reached at 20 000 G, the Hall factor approaches unity in this temperature region. Figures 3 and 4 show the measured mobilities for phosphorus-doped samples (except Si: P 6); and

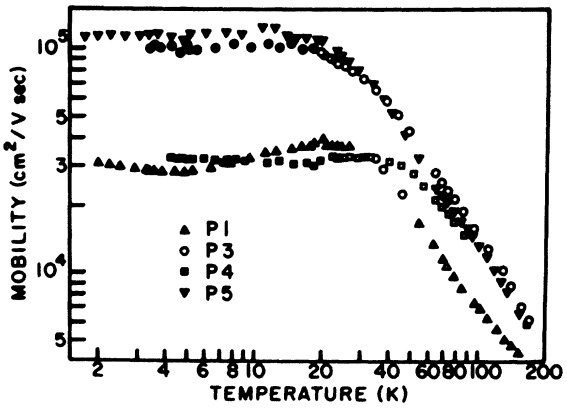

FIG. 3. Mobilities as measured for four phosphorus-doped silicon samples. Sample properties are listed in Table I. Open data points are measured with thermal carrier generation. Solid data points are taken with the sample illuminated with 300-K background radiation (photo-Hall effect).

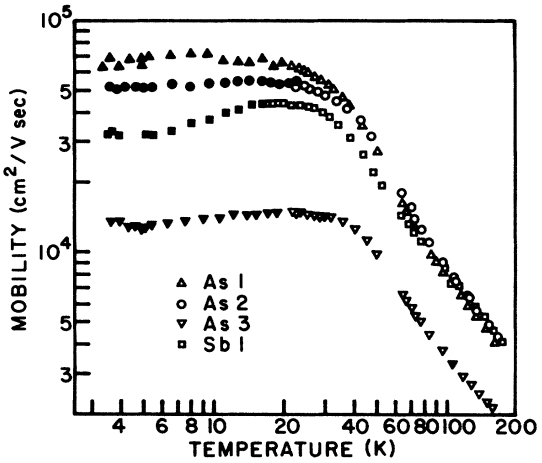

FIG. 4. Mobilities as measured for three arsenic-doped and one antimony-doped silicon samples.

for arsenic- and antimony-doped samples. A rough estimate of the high-field limit region is found from the condition on the mobility-field product $\mu B > 1\times10^{8}$ G cm^2/V sec. Section III deals directly with the mobility analysis of these samples. We now present the theory and results of the analysis of carrier concentration as a function of temperature.

The twelvefold (including spin) 1S state of group-V donors[14,15] in silicon is split into a twofold-degenerate ground state, 1S (A_1), and two groups of higher states, 1S (T_1) and 1S (E). In addition, excited states of these impurities lie closer to the band edge. Kohn[14] has calculated the excited-state energy levels and degeneracies, while the 1S-state splittings have been measured by Aggarwal.[16]

These energy states are related to the carrier concentration n, donor and acceptor densities N_d and N_a, and the density of states in the conduction band N_c, as[17,18]

$$\frac{n(n+N_a)}{N_d-N_a-n} = \frac{N_c e^{-E_d/kT}}{2+6e^{-D/kT}+4e^{-(D+d)/kT}+e^{-E_d/kT}\sum_i g_i e^{E_i/kT}}, \tag{2}$$

where E_d is the energy of the ground state [1S(A_1)], D and d are the 1S-state splittings,[16] and E_i and g_i refer to the energy and degeneracy of the excited states. We have included three groups of excited states, near 10, 6, and 3 meV. Thus

$$\sum_i g_i e^{E_i/kT} = 24e^{0.0102/kT} + 36e^{0.0058/kT} + 24e^{0.0029/kT}. \tag{3}$$

Equation (2) was used to determine N_d, N_a, and E_d by fitting the measured temperature dependence of the carrier concentration in a manner described elsewhere.[10] N_c was taken to be $5.29\times10^{15}T^{3/2}$ cm^{-3}, as calculated for a density-of-states effective mass of $0.32m_0$.

The results of fitting the carrier concentration as a function of temperature to Eq. (2) for the various samples are presented in Table I. With two exceptions, we have fixed the value of N_c and only varied N_d, N_a, and E_d. In the case of our two purest samples, Si: P 5 and Si: P 6, we have also fit them with N_c variable, and both results are shown in Table I. As can be seen, there is very little change in any of the parameters when N_c is permitted to vary. This was not necessarily the case in the less pure samples, for which the exhaustion region ($n \simeq N_d - N_a$) was not reached be-

TABLE I. Carrier-concentration-analysis results for samples fit to Eq. (2).

Sample	N_d (cm^{-3})	N_a (cm^{-3})	E_d (meV)	$N_c/T^{3/2}$ ($K^{-3/2}$ cm^{-3}) (10^{15})	m^*/m_0	Resistivity at 300 K (Ω cm)	Stand dev. of fit (10^{-2})
Si: P 1	9.5×10^{15}	4.2×10^{12}	45.64	5.29[a]	0.3218[a]	0.66	4.17
Si: P 3	2.5×10^{14}	2.3×10^{13}	45.14	5.29[a]	0.3218[a]	17.1	0.55
Si: P 4	9.6×10^{14}	2.0×10^{14}	43.39	5.29[a]	0.3218[a]	4.76	1.02
Si: P 5	3.3×10^{14}	8.6×10^{12}	45.38	5.29[a]	0.3218[a]	13.6	0.56
	3.3×10^{14}	8.6×10^{12}	45.33	5.18	0.3175	13.6	0.57
Si: P 6	4.3×10^{13}	7.7×10^{12}	45.42	5.29[a]	0.3218[a]	123.	0.61
	4.3×10^{13}	7.1×10^{12}	45.42	4.82	0.3026	123.	0.48
Si: As 1	1.4×10^{16}	6.0×10^{12}	53.64	5.29[a]	0.3218[a]	0.43	2.75
Si: As 2	7.9×10^{15}	4.3×10^{13}	52.54	5.29[a]	0.3218[a]	0.66	1.88
Si: As 3	7.5×10^{16}	1.8×10^{13}	52.52	5.29[a]	0.3218[a]	0.13	5.36
Si: Sb 1	7.4×10^{15}	5.3×10^{12}	42.59	5.29[a]	0.3218[a]	0.68	2.53

[a]Value fixed.

low 160 K.

In several of the more impure samples having donor concentrations of about 10^{16} cm^{-3} or more, we have also tried fits with one or more data points taken at 300 K. In this case the value of n at 300 K was calculated by several methods. First, the measured resistivity was used to give a value of N_d from the graph published by Irvin.[19] Using the appropriate activation energy, we calculated n/N_d at 300 K and obtained a value of n by multiplying this ratio by N_d. The second method used the Hall coefficient measured in the low-field limit at 300 K, and corrected by the Hall factor calculated from Eq. (1), to give a value of n. The third method used the measured Hall coefficient and the Hall mobility at 300 K. Instead of calculating the Hall factor from Eq. (1), the drift mobility was calculated and the ratio of Hall to drift mobility was used as the Hall factor to correct the Hall coefficient. All three methods gave similar results, although the first and third rely on good geometry[20] for an accurate measure of the resistivity. Adding a data point at 300 K had only a slight effect on the fit, for example, Si: As 1 showed at most a 5% decrease in N_d and an 8% increase in N_a from the values obtained without a data point above 160 K. This check provides reasonable confidence in extrapolating the fitting procedure to samples for which the exhaustion region could not be measured in the high-field limit.

III. MOBILITY ANALYSIS

A. General Formulation

We have analyzed the mobility in these same samples in order to determine the density of compensating acceptors N_a and the values of various other parameters associated with the scattering mechanisms. N_a can be deduced from the strength of ionized-impurity scattering, especially at low temperatures where $n \ll N_a$ and lattice scattering is relatively weak. To do this, however, one needs to have an accurate description not only of ionized-impurity scattering in a many-valley band structure, but also lattice and neutral-impurity scattering. The anisotropy of the effective mass in silicon produces different scattering rates for the transverse and longitudinal directions in the ellipsoidal valley. Since each scattering process has a different dependence on the effective mass of the carriers, it is not possible to select an average effective mass suitable for all three types of scattering. We have separated the scattering time averages into two parts, as generally prescribed by Herring and Vogt,[1] and as done by Brooks[2] in treating lattice scattering for ellipsoidal bands. This type of treatment is valid when the scattering is either energy conserving or momentum randomizing. The mobility in this case can be written

$$\mu = \tfrac{1}{3} e \left[\langle \tau_{\parallel} \rangle / m_{\parallel}^{*} + 2(\langle \tau_{\perp} \rangle / m_{\perp}^{*}) \right] , \tag{4}$$

where $\parallel$ and $\perp$ refer to the longitudinal and transverse directions, respectively. Each average of the scattering time is computed numerically by approximating

$$\langle \tau \rangle = (4/3\sqrt{\pi}) \int_0^{\infty} e^{-x} x^{3/2} \tau(x)\, dx \tag{5}$$

with Simpson's rule, where $x = \epsilon/kT$. In using Simpson's rule we have taken the integral from 0 to $25kT$, and used 75 intervals; or used two regions, from 0 to $6kT$ with 24 intervals and 6 to $25kT$ with 19 intervals. The accuracy of the numerical integration using these choices was compared with taking the integral from 0 to $25kT$ in 500 intervals. Over the temperature range from 5 to 500 K, the maximum error was 1.75% (at 500 K, $N_d = 1\times10^{15}$ cm^{-3}, $N_a = 1\times10^{10}$ cm^{-3}) in the first case with one region; and 1.13% (at 300 K, $N_d = 1\times10^{15}$ cm^{-3}, $N_a = 1\times10^{10}$ cm^{-3}) in the second case with two regions. For these comparisons we used hypothetical samples with a range of donor concentrations from 10^{10} to 10^{17} cm^{-3}, having only a small amount of compensation. Since the error was almost always less with the two region integration, we used it in preference to the single region. This was also considerably faster.

The lattice scattering mechanism in n-type silicon has been the subject of much recent discussion. Electron scattering mechanisms by lattice modes are of two types: intravalley scattering by acoustic phonons, and intervalley scattering to either parallel valleys (g type) or perpendicular valleys (f type). The allowed intervalley modes have recently been agreed upon, at least theoretically, although certain experimental evidence suggesting possible scattering by forbidden intervalley modes remains to be explained. We will discuss this later Sec. IV C. In general, the transverse lattice scattering time can be written

$$\frac{1}{\tau_{L\perp}} = \frac{1}{\tau_0 T^{-3/2} x^{-1/2}} \left(1 + \sum_i \{ w_i (\theta_i/T) [n_i (1 + \theta_i/Tx)^{1/2} + (n_i + 1)(1 - \theta_i/Tx)^{1/2}] \} \right) , \tag{6}$$

where θ_i is the temperature of the ith intervalley phonon, $n_i = [\exp(\theta_i/T) - 1]^{-1}$, and w_i is the relative coupling strength of the electrons to the ith intervalley mode compared to the transverse acoustic mode. Long and Myers[21] determined the ratio of the acoustic mode scattering strength in the longitudinal direction to be $\frac{2}{3}$ that of the transverse direction. This has been confirmed by Neuringer and Little[22]

also using magnetoresistance measurements, and by recent experiments involving cyclotron resonance of hot electrons as measured by Kazanskii and Koshelev.[23] Intervalley scattering is assumed to be isotropic. Therefore, the scattering time in the longitudinal direction is

$$\frac{1}{\tau_{L\parallel}} = \frac{1}{\tau_{L\perp}} + \frac{1}{2\tau_0 T^{-3/2} x^{-1/2}} \quad . \tag{7}$$

Neutral-impurity scattering has been calculated from Erginsoy's[8] expression derived from the study of low-energy elastic scattering of electrons from hydrogen. In the zero-order phase-shift approximation, this type of scattering is independent of carrier energy. However, it has been shown that for large concentrations of neutral impurities, coherent scattering can take place,[10,24,25] so that the scattering time may not depend directly on the inverse neutral donor concentration. Also, group-V donors in silicon are not strictly hydrogenic. Therefore, we have scaled the neutral-impurity scattering time with an adjustable constant A to be determined from the analysis of the data. With this provision, the neutral-impurity scattering time is

$$\frac{1}{\tau_N} = \left(\frac{\kappa\hbar^2}{m_g^* e^2}\right)\left(\frac{20\hbar}{m_c^*}\right)\frac{N_N}{A} = \frac{4.57\times10^{-6}}{(m_c^*/m_0)A} N_N \,, \tag{8}$$

where $N_N = N_d - N_a - n$ is the density of neutral donors, m_c^* is the effective mass of the conduction electron ($m_\perp^*$ or $m_\parallel^*$), and m_g^* is the geometric mean mass which for silicon is $0.32 m_0$.

Ionized-impurity scattering has been calculated by Brooks,[2] Herring, and Dingle.[3] This formula has been quite successful in describing ionized-impurity scattering in both silicon[12] and germanium.[10] The ionized-impurity-scattering time is

$$\frac{1}{\tau_I} = \frac{N_I \pi e^4}{(kT)^{3/2}\kappa^2 (2m_c^*)^{1/2} x^{3/2}} [\ln(b+1) - b/(b+1)]$$

$$= \frac{1.68\times10^{-2} N_I}{T^{3/2}(m_c^*/m_0)^{1/2} x^{3/2}} [\ln(b+1) - b/(b+1)], \tag{9}$$

where

$$b = \frac{2\kappa m_c^* (kT)^2 x}{\pi\hbar^2 e^2 n'} = \frac{5.17\times10^{14}(m_c^*/m_0) T^2 x}{n'} \tag{10}$$

and

$$n' = n + (n+N_a)[1 - (n+N_a)/N_d] \,. \tag{11}$$

N_I is the total density of ionized impurities, namely, $2N_a + n$.

A somewhat less known treatment of ionized-impurity scattering given by Samoilovich *et al*[4-6] has also been evaluated. The theory, similar to earlier work by Ham,[26] specifically treats anisotropic ionized-impurity scattering in a prolate spheroical band. Neuringer and Long[27] have interpreted magnetoresistance data with respect to the relative ratio of longitudinal to transverse scattering time predicted from the theory, but we do not know of any reference dealing with the absolute magnitudes of the scattering times as predicted by Samoilovich *et al*. The expressions given here have been evaluated specifically for n-type silicon, and the reader is referred to the original papers for a complete description. With $b_\parallel$ evaluated as in Eq. (10), ($m_c^* = m_\parallel^*$), we find

$$\frac{1}{\tau_{I\perp}} = \frac{4.28\times10^{-2} N_I}{(Tx)^{3/2}(1+g_1)} [\ln(b_\parallel) - 2.34 + 7.88/b_\parallel], \tag{12}$$

$$\frac{1}{\tau_{I\parallel}} = \frac{1.18\times10^{-2} N_I}{(Tx)^{3/2}(1+g_0)} [\ln(b_\parallel) - 1.75 + 4.64/b_\parallel], \tag{13}$$

where g_0 and g_1 have been given graphical representation in Ref. 4. We have approximated these by the following expressions:

$$g_0 = 0.192 - 0.067[5/\log_{10}(b_\parallel)] \,, \tag{14}$$

$$g_1 = 0.03[\log_{10}(b_\parallel) - 1] \,. \tag{15}$$

Since these functions are small corrections, we have evaluated g_0 and g_1 outside the integral, calculating $b_\parallel$ in this case from Eq. (10) using $x = 3$.

The total scattering time to be averaged in Eq. (5) is defined

$$\tau(x) = \left(\frac{1}{\tau_L} + \frac{1}{\tau_N} + \frac{1}{\tau_I}\right)^{-1} , \tag{16}$$

where the transverse and longitudinal averages are computed as required in Eq. (4).

Before going ahead to the results of the analysis, it is important to note that none of the several scattering mechanisms can be totally isolated in realistic material. Therefore, the results presented in Secs. III B–III D dealing with a particular scattering mechanism will have interacted with each other during the several months taken to complete this work. These interactions were always present, and although we cannot describe them totally, it is hoped that this remark will explain why minor modifications appear, for example, in the choice of A, during the development of our treatment of lattice scattering.

B. Lattice Scattering Results

Having presented the formulation of the mobility calculation, we must evaluate the lattice scattering parameters τ_0 and the w_i's given in Eqs. (6) and (7). We initially used the model proposed by Rode,[28] model I, with only one intervalley phonon ($\theta_1 = 540$ K). Therefore, the parameters calculated by Long[7] could not be adopted, since his model assumed two intervalley phonons with temperatures 630 and 190 K. Also, the mobility due to pure lattice scattering is not clearly established in the literature. Mea-

sured mobilities range from 18 000 to 24 000 $cm^2/V sec$ at 77 K,[28] with additional uncertainties arising when the Hall factor and impurity scattering must be taken into account. We decided initially to determine τ_0 from the data taken on our two purest samples, by fitting τ_0 as a parameter using data from 20 to 77 K.[29] Both of these samples, Si : P 5 and Si : P 6, were cut with bridge shapes favorable to an accurate determination of the distance and width between resistivity arms, so that geometrical errors should be small.[30] For this fit, w_1 was fixed at 1.5 (w_{2-4} were fixed at zero) and since intervalley scattering lowers the mobility by less than 3% for this model at 77 K, this choice was unimportant. We found good agreement for both samples, using several trials with parameters N_a and A both fixed and variable. Using the temperature range from 77 K down, we found τ_0 to be 3.56×10^{-9} sec, within 1.7%. In addition, we ran a second series of fits with data from a more restricted temperature range, 20–41 K. The average values of τ_0 were 2.7% and 1.1% higher for samples Si : P 5 and Si : P 6, respectively, when only data from below 41 K was used. With τ_0 chosen to be 3.56×10^{-9} sec, we then ran a series of calculated mobilities at 300 K, varying w_1. From this series, we selected w_1 to agree with the measured drift mobility at 300 K. Drift-mobility experiments[31–34] give mobilities between 1350 and 1500 $cm^2/V sec$ at room temperature. We chose to use $w_1 = 1.45$, giving a mobility of about 1450 at 300 K, consistent with our own measurements which will be described later.

The two temperature ranges used above to determine τ_0 were chosen deliberately to see if there was a significant amount of intervalley scattering by lower temperature phonons (LA g type or TA f type) as suggested by several authors, but forbidden by the calculated selection rules. If lower temperature phonons were contributing significantly, we would expect the fitted values of τ_0 to be higher using data from the temperature range below 41 K. Also, the fit would be skewed when the temperature range up to 77 K was used, since the adjustment of τ_0 alone could not compensate for a low-temperature intervalley mode. Although there is only a slight increase in the average value of τ_0 using only data below 41 K, the fit over the 20–77-K range remained slightly skewed even when N_a and A were permitted to vary. Also, fitted values of N_a were lower when the full range of 20–77 K was used, indicating an adjustment of N_a in attempt to raise the mobility at low temperatures with respect to higher temperatures. This discrepancy, although not prominent, indicated a possible weak contribution from a low-temperature intervalley phonon.

At this point in our work it became apparent that more complete data at higher temperatures would be necessary to characterize the intervalley scattering process. We therefore extended the range of measurements on our purest sample, Si : P 6, to room temperature, measuring the Hall constant at both 600 and 20 000 G, along with the resistivity. Since the analysis of carrier concentration could be carried out with data taken below 100 K for this sample, the carrier concentration above 100 K could be accurately calculated from the values of N_d, N_a, and E_d as given in Table I. From this, we deduced the Hall factor and mobility up to room temperature, without relying on Eq. (1) which assumes an accurate knowledge of the scattering times. Data taken between 77 and 315 K were then compared to model I, which we will now call model I(a). Deviations between the data and model I(a) were skewed by 5 to 6%. Two modifications were then attempted on model I. First, we tried using a phonon temperature of 670 K rather than 540 K [model I(b)]. For this choice a coupling constant of 2.0 was needed to give agreement to drift mobility at 300 K. Comparison with our data above 77 K again gave deviations on the order of 6%. Next, we used a combination of both these intervalley phonons, $\theta_1 = 540$ K and $\theta_2 = 670$ K [model I(c)]. By computer adjustment of w_1 and w_2, the maximum error was reduced to about 3% over the temperature range above 77 K.

Having exhausted the possibilities of model I, we returned to the low-temperature region below 77 K to see if a low-temperature phonon would appreciably improve the fit in this region. A second model, model II, was calculated using a low-energy phonon corresponding to f-type scattering by a TA phonon, in addition to the allowed higher temperature phonons. For this series we fixed w_1 and w_2 at 0.6 and 1.2, respectively, as determined from model I(c) fit above 77 K. Using data from 20 to 77 K, and with θ_3 chosen to be 190 K,[7] we fit both τ_0 and w_3, with N_a both fixed and variable. Good agreement was again obtained between samples Si : P 5 and Si : P 6, and the results of fits below 77 K are given in Table II, together with the standard deviations. The marked improvement in the standard deviation when the forbidden intervalley phonon was included is good evidence of its importance, even though it is weakly coupled. Figures 5 and 6 illustrate the relative error between measured and calculated mobilities for these two samples, with and without the addition of a low-temperature intervalley phonon.

With the importance of a low-energy phonon established, we again went to the temperature region above 77 K and fit model II with τ_0, w_1, and w_2 variable. With this freedom, agreement was obtained to better than 2%, with the coupling constant of w_1 fitted to essentially zero ($w_1 < 0.001$), and w_2 fit to about 1.9. Since w_3 was fixed at 0.15

TABLE II. Mobility latttice parameters fit below 77 K.

Model	Sample	τ_0 (sec^{-1}) (10^{-9})	w_1 [a,b]	w_2 [a,b]	w_3 [b]	A	N_a (cm^{-3}) (10^{12})	Stand. dev of mobility fit (10^{-2})	Temperature range (K)
I	Si: P 5	3.57	1.5	0	0[a]	5.9	9.2	5.37	20–77
I	Si: P 5	3.57	1.5	0	0[a]	5.3	8.6[a]	4.02	20–77
I	Si: P 5	3.62	1.5	0	0[a]	2.0[a]	6.0	1.04	20–77
I	Si: P 6	3.54	1.5	0	0[a]	14.2	6.2	2.35	20–77
I	Si: P 6	3.55	1.5	0	0[a]	30.5	7.7[a]	5.23	20–77
I	Si: P 6	3.53	1.5	0	0[a]	2.0[a]	5.3	1.43	20–77
I	Si: P 5	3.62	1.5	0	0[a]	4.8	8.6[a]	4.47	20–41
I	Si: P 5	3.69	1.5	0	0[a]	2.0[a]	6.5	0.32	20–41
I	Si: P 6	3.60	1.5	0	0[a]	25.5	7.7[a]	6.44	20–41
I	Si: P 6	3.60	1.5	0	0[a]	2.0[a]	5.8	0.25	20–41
II	Si: P 5	3.99	0.6	1.2	0.17	2.0[a]	8.6[a]	1.21	20–77
II	Si: P 5	3.79	0.6	1.2	0.08	2.0[a]	7.0	0.48	20–77
II	Si: P 6	3.92	0.6	1.2	0.19	2.0[a]	7.7[a]	1.33	20–77
II	Si: P 6	3.73	0.6	1.2	0.10	2.0[a]	6.3	0.73	20–77

[a]Value fixed.

[b]Coupling constants for intervalley phonons; $\theta_1 = 540$ K, $\theta_2 = 670$ K, $\theta_3 = 190$ K.

during this fit, the result is identical to that determined by Long,[7] except for a slight difference in the value of θ_3. Very little change was observed when all four variables (τ_0, w_1, w_2, and w_3) were permitted to vary, and data between 20 and 315 K was used. Results in the higher-temperature region are summarized in Table III.

At this time it had become evident not only from these samples, but also from more heavily doped ones, that ionized-impurity scattering as calculated from the expression given by Brooks, Herring, and Dingle [Eqs. (9)–(11)] was overestimating the ionized-impurity-scattering strength and that consequently whenever N_a was permitted to vary, values considerably smaller than those determined in Sec. II were obtained. Therefore, the ionized-impurity-scattering formulas given by Samoilovich *et al.* were substituted [Eqs. (12)–(15)] after it was clear that they gave a substantial improvement. We also decided to include the possibility of a fourth intervalley phonon with a characteristic temperature of 307 K, (this would be LA g-type, but not quite at 0.34X as expected) as inferred from optical measurements.[35] These changes defined what we shall call model III. With N_a, τ_0, and four w_i's variable, we fit the data on Si: P 6 between 20 and 315 K. Only w_2 and w_3 ($\theta_2 = 670$ K, $\theta_3 = 190$ K) were found to be important, but now N_a fit very close to the value determined in Sec. II. We also fit Si: P 5 between 20 and 77 K, varying N_a, τ_0, w_3, and w_4. Again, w_4 was found to be unimportant and N_a fit very close to the result for this sample found in Sec. II. Model-III results are summarized in Table IV for these two samples, and the relative errors are shown in Figs. 7 and 8.

As an additional check on our results, we calculated the Hall factor for Si: P 6 using Eq. (1) and with parameters determined from several models. These are compared to our data taken at 600 and 20 000 G between 77 and 315 K, as shown in Fig. 9. None of the models gives completely satisfactory agreement, with model III giving the best results below 100 K, and model I(a) giving the best agreement from 100 to about 250 K. It should be noted that the data taken at 20 000 G will not be

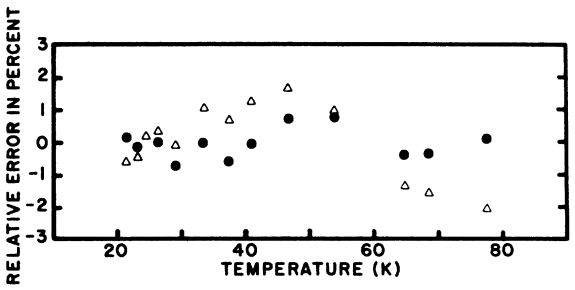

FIG. 5. Relative error in percent between calculated and measured mobility for Si: P 5 with and without the inclusion of a low-temperature intervalley phonon ($\theta_3 = 190$ K). The relative error is defined as Error $= [(\mu_m - \mu_c)/\mu_m] \times 100$, where μ_m is the measured mobility, and μ_c is the calculated mobility. The open triangles show the result without the inclusion of θ_3. The solid circles show the improved fit with θ_3 included. Values of parameters are the following: fixed, $N_d = 3.28 \times 10^{14}$, $A = 2.0$, $G = 1.0$, $w_1 = 0.6$, $w_2 = 1.2$; fit, open triangles, $N_a = 5.9 \times 10^{12}$, $\tau_0 = 3.62 \times 10^{-9}$ ($\omega_3 = 0.0$ fixed); fit, solid circles, $N_a = 7.0 \times 10^{12}$, $\tau_0 = 3.79 \times 10^{-9}$, $w_3 = 0.08$.

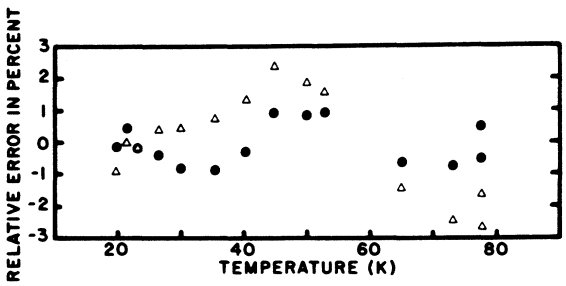

FIG. 6. Relative error as in Fig. 5, for sample Si: P 6. Values of the parameters are the following: fixed, $N_a = 4.29\times10^{13}$, $A = 2.0$, $G = 1.0$, $w_1 = 0.6$, $w_2 = 1.2$; fit, open triangles, $N_a = 5.3\times10^{12}$, $\tau_0 = 3.53\times10^{-9}$ ($\omega_3 = 0.0$ fixed); fit, solid circles, $N_a = 6.3\times10^{12}$, $\tau_0 = 3.73\times10^{-9}$, $w_3 = 0.10$.

in the low-field limit below 150 K.

In conclusion, we show in Fig. 10 the experimental data on Si: P 6, including photo-Hall data omitted from the fitting procedure, together with the calculated mobility curve based on model III.

C. Ionized-Impurity-Scattering Results

Ionized-impurity scattering has been treated using the expression given by Brooks, Herring, and Dingle in most of the recent experimental[10,12,36,37] and theoretical[28] work on this subject. However, as has been mentioned in Sec. III B, the agreement in fitting N_a was less than satisfactory for our purest samples Si: P 5 and Si: P 6 when the expression given by these authors was used. It was also tried on several more heavily doped samples, having stronger contributions due to ionized-impurity scattering. The values of N_a which were fit from this formula were about 30% lower in all cases than those determined from the carrier-concentration analysis given in Table I. Consequently, we also ran fits using the ionized scattering formula given by Samoilovich *et al*, and the results were much better. A comparison of the two results is given in Table V. The most sensitive samples for this comparison are Si: P 3 and Si: P 4, which have the largest contributions due to ionized impurities, and relatively weak contributions due to neutral scattering. Several values of the neutral scattering parameter A were tried, to verify that the fitted value of N_a did not depend upon this choice. As a counterexample, the choice of A is more important for Si: As 2, which has a fairly strong contribution due to neutral-impurity scattering. In all cases, however, the formulas given by Samoilovich *et al.* gave better agreement in determining values of compensation close to those determined from carrier-concentration analysis.

D. Neutral-Impurity-Scattering Results

Having established a reasonably good model to describe the lattice and ionized-impurity-scattering effects, we then went on to fit the remaining samples which were lightly compensated, and hence had substantial contributions due to neutral-impurity scattering. The results were disappointing. In all cases the fits between 20 and 77 K were skewed, with the calculated mobility higher at the extremes and lower than the measured mobility between about 25 and 60 K. In these samples, N_a was fixed and A and G [30] were permitted to vary. For completeness, the results of these fits are given in Table VI.

In order to understand the cause of the poor fitting, we have extracted the neutral scattering contributions from each of these samples for comparison with the Erginsoy model. To do this we calculated the mobility for each of these samples, including only the contributions due to lattice and ionized-impurity-scattering effects, with G assumed to be unity. We then estimated the neutral-scattering mobility as

$$\mu_N = (1/\mu_{\text{meas}} - 1/\mu_{L+I\ \text{calc}})^{-1} . \tag{17}$$

TABLE III. Mobility lattice parameters fit above 77 K.

Model	Sample	τ_0 (sec^{-1}) (10^{-9})	w_1[a]	w_2[a]	w_3[a]	Stand. dev of mobility fit (10^{-2})	Temperature range (K)
I(*a*)	Si: P 6	3.56[b]	1.45	0[b]	0[b]	...[c]	77–315
I(*b*)	Si: P 6	3.56[b]	0[b]	2.00	0[b]	...[c]	77–315
I(*c*)	Si: P 6	3.56[b]	0.58	1.19	0[b]	1.21	77–315
II	Si: P 6	3.90[b]	0.00	1.90	0.15[b]	1.02	77–315
II	Si: P 6	3.92	0.00	1.93	0.15[b]	1.02	77–315
II	Si: P 6	3.89	0.01	1.87	0.15	1.39	20–315

[a]Coupling constants for intervalley phonons; $\theta_1 = 540$ K, $\theta_2 = 670$ K, $\theta_3 = 190$ K.
[b]Value fixed.
[c]Not computer fit.

TABLE IV. Mobility lattice parameters fit with model III.

Sample	τ_0 (sec^{-1}) (10^{-9})	w_1[a]	w_2[a]	w_3[a]	w_4[a]	N_a (cm^{-3}) (10^{12})	Stand. dev. of mobility fit (10^{-2})	Temperature range (K)
Si: P 6	3.63	0.0002	1.84	0.080	0.0004	7.56	0.90	20–315
Si: P 5	3.77	0.0[b]	1.83[b]	0.16	0.00007	8.40	0.47	20–77

[a]Coupling constants for intervalley phonons; $\theta_1 = 540$ K, $\theta_2 = 670$ K, $\theta_3 = 190$ K, $\theta_4 = 307$ K.
[b]Value fixed.

For comparison, the mobilities calculated in this manner were multiplied by the total concentration of neutral impurities at each temperature. In addition, we repeated the same procedure, replacing the measured mobility by the mobility calculated with the inclusion of neutral scattering from Erginsoy's formula. For this calculation a value of A was used, as indicated from our results given in Table VI, and three choices of G were assumed: 0.95, 1.0, and 1.05, corresponding to hypothetical errors in the sample geometry. Since Erginsoy predicts a temperature-independent mobility, our calculated mobility including neutral scattering was used to check if the above procedure recovered this temperature-independent behavior out of the involved averaging of scattering times. By also varying G, we could estimate the reliability of the procedure in view of probable errors in geometry, and observe the consequences of such errors.

We have included in this procedure both Hall and photo-Hall data, the latter being taken at temperatures between 1.5 and 20 K with 300-K background radiation. Lower temperature bounds for the validity of this data arise in two ways. First, the condition of the Born approximation used in calculating the ionized-impurity-scattering contribution means that we must have $|\vec{k}a| \gg 1$,[38] where $\vec{k}$ is the carrier wave number and a is the scattering length. For silicon, this becomes $|\vec{k}a| \gg 1.28\times10^7 T(m^*/n')^{1/2}$, with n' given by Eq. (11). The second requirement for these data to be valid is that the thermalization time of the photoexcited carriers must be much shorter than the carrier lifetime. Carrier lifetimes were determined for most of these samples from the decay of the photoresponse to a pulsed CO_2 laser. The results of these measurements have been published.[39] We can estimate the thermalization time for electrons in n-type silicon from the energy loss rate due to acoustic phonon emission.[40] In all cases, the greatest lower bound in temperature is determined by considering the problem of thermalization time in comparison to lifetime. Data were used only for temperatures above $2T'$, where T' is the temperature at which the lifetime and thermalization times are equal, as determined for each sample.

Figure 11 shows the results found for Si: P 1. As can be seen, the strength of neutral scattering decreases slightly from around 5 to 50 K, and then increases rather sharply above 50 K, causing the mobility (per scattering center) to decrease. For comparison, the calculated results found from the same procedure using the expression for neutral scattering given by Erginsoy are also shown. As expected, very little temperature dependence is evident in the calculated curves, except at the highest temperatures for those cases with hypothetical errors in sample geometry. It should be noted that in no case will a fixed geometrical error yield a temperature dependence similar to our experimental results. It is also clear why the computer fits between 20 and 77 K were high at the extremes and low between about 25 and 60 K, as we have stated.

Figures 12–16 give the same information for samples Si: P 5 (marginal amounts of neutral scattering), Si: As 1, Si: As 2, Si: As 3, and Si: Sb 1.

Two conclusions can be drawn by comparing these figures. First, a general pattern of increasing mobility up to about 50 K is seen, followed by a decrease from 50 to 100 K. Second, the average mobility for the arsenic-doped samples was substantially larger than that of either phosphorus- or antimony-doped samples. These conclusions will be discussed in Sec. IV E.

IV. COMPARISON WITH THEORY AND OTHER EXPERIMENTS

A. Carrier Concentration Analysis

The principal advantage of our work over the earlier analysis of Long and Myers[12] is that here

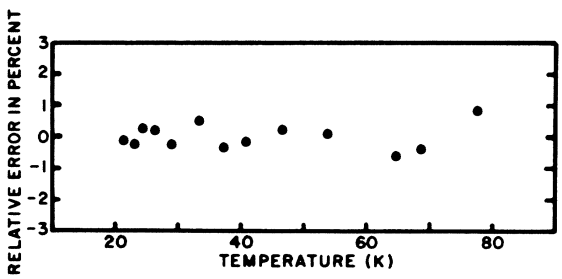

FIG. 7. Relative error for Si: P 5, with model III. Values of the parameters are listed in Table IV.

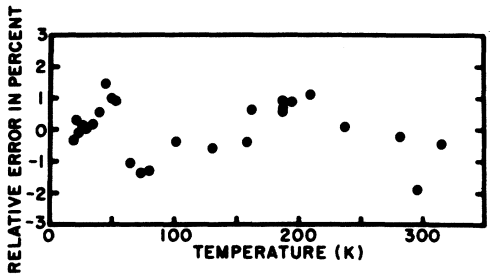

FIG. 8. Relative error for Si: P 6, with model III. Values of the parameters are listed in Table IV.

no iterative procedure was necessary to determine Hall-factor corrections, since our data were taken in the high-field limit. This independence of the carrier-concentration analysis with respect to the mobility analysis has allowed the two methods to be compared, rather than seeking a self-consistent fusion of the analysis as done by Long and Myers.

All of the samples were analyzed with an activation energy which was assumed to be independent of doping concentration and temperature. This approximation is valid at low temperatures for lightly doped samples without a large number of compensating acceptors. For more heavily doped samples, approaching the exhaustion region will appreciably lower the activation energy, although it should be noted that the dependence of carrier concentration on activation energy in this region is not strong. Early measurements by Pearson and Bardeen[41] and more recently by Penin *et al.*[42] have been analyzed,

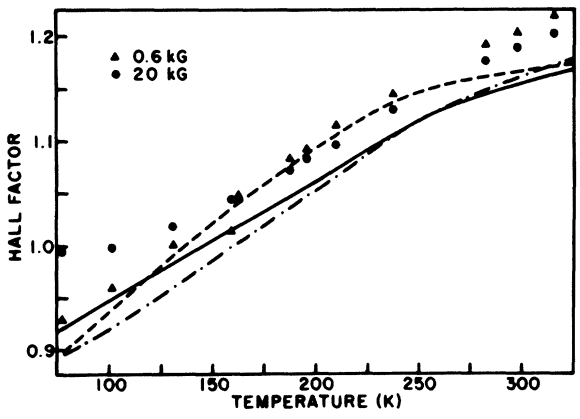

FIG. 9. Hall factor, as measured at 600 and 20 000 G for Si: P 6. Data taken with 20 000 G were not in the low-field limit below about 150 K. Calculated curves of the Hall factor are model 1(a) shown as dashed line, model 1(b) shown as dash-dot line, model III shown as solid line. Parameters used for the calculation are given in Tables III and IV.

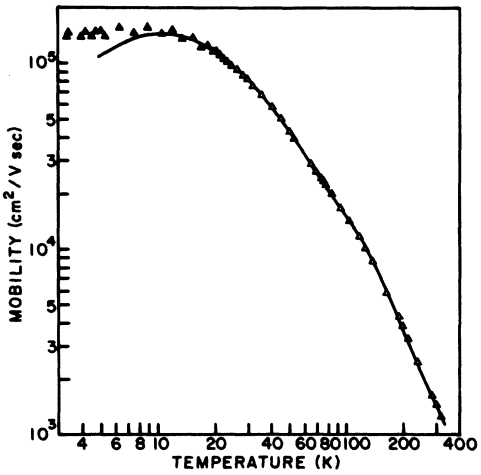

FIG. 10. Experimental data points and calculated mobility curve for Si: P 6. Experimental data include photo-Hall measurements (solid circles) below 20 K which were not included in the fitting procedures. Deviation between the data and calculation below 10 K occurs because the photoexcited carriers are no longer able to completely thermalize at the lowest temperatures. Parameters from Table III are used for the calculation. Figure 8 shows the details of the difference between calculation and data above 20 K.

following Debye and Conwell[43] with the activation energy assumed to be related to the total ionized impurity concentration $N_I = 2N_a + n$ as

$$E_d = E_d(0) - \alpha N_I^{1/3}, \tag{18}$$

where α was determined by Penin *et al.* to be 3.6×10^{-6} eV cm, giving an activation energy of zero for phosphorus impurities at a concentration of 2×10^{18} cm^{-3}. If we use this value of α to compute the lowering of the activation energy in the freeze-out region for our purest samples, Si: P 5 and Si: P 6, with about 8×10^{12} cm^{-3} acceptors, we find a calculated shift of nearly 1 meV. If we add this to the values of E_d determined in Table I for these samples, we find $E_d(0)$ to be about 46.3 meV. Since this is larger than the optical activation energies found by Aggarwal and Ramdas[44] in accordance with the recent theory of Faulkner[45] (45.53 meV), there is some doubt as to the validity of Eq. (18) at these low concentrations. Penin *et al.* also give an expression for the variation of E_d with the principal dopant density, and this gives negligible reduction in activation energy for these lightly doped samples, since it involves a term proportional to e^{-r_d/a^*}, where r_d is the average spacing between donors, namely, $r_d = (3/4\pi N_d)^{1/3}$, and a^* is the effective Bohr radius. Another approach, taken by Neumark,[46] basically involves the effect of screening by impurities on the activation energy. This depends only on the ionized-

TABLE V. Comparison of the compensation densities fit from two different formulas for ionized-impurity scattering, as given by Brooks, Herring, and Dingle (BHD) and by Samoilovich *et al.* (SKDI).

Sample	N_a from carrier-conc. analysis (cm^{-3})	N_a from mobility analysis (cm^{-3})	Theory	A	G	Stand. dev. of fit (10^{-2})
Si: P 3	2.3×10^{13}	1.49×10^{13}	BHD	1.6[a]	1.12	1.5
		1.53×10^{13}	BHD	2.0[a]	1.12	1.5
		1.55×10^{13}	BHD	2.4[a]	1.12	1.5
		2.04×10^{13}	SKDI	1.6[a]	1.12	1.1
Si: P 4	2.0×10^{14}	1.43×10^{14}	BHD	1.6[a]	1.12	0.5
		1.46×10^{14}	BHD	2.0[a]	1.12	0.5
		1.49×10^{14}	BHD	2.4[a]	1.12	0.5
		1.93×10^{14}	SKDI	1.6[a]	1.13	0.7
Si: P 5	8.6×10^{12}	6.97×10^{12}	BHD	2.0[a]	1.00[a]	0.5
		8.40×10^{12}	SKDI	1.6[a]	1.00[a]	0.5
Si: P 6	7.7×10^{12}	6.32×10^{12}	BHD	2.0[a]	1.00[a]	0.7
		7.56×10^{12}	SKDI	1.6[a]	1.00[a]	0.9
Si: As 2	4.3×10^{13}	2.52×10^{13}	BHD	5.3[a]	1.04	1.2
		3.02×10^{13}	SKDI	5.3[a]	1.01	1.9
		5.20×10^{13}	SKDI	31	0.95	1.0

[a]Value fixed.

impurity concentrations, to first order, and gives a reduction in the activation energy of approximately 0.3 meV at 30 K for phosphorus impurities with sample concentrations representative of Si: P 5 and Si: P 6. Even this modest decrease in activation energy is sufficient to imply a value of $E_d(0)$ greater than the optical results, although the discrepancy is certainly small. In spite of the uncertain nature of these calculations, we compare in Table VII the value of $E_d(0)$ calculated from Eq. (18) and from the expression given by Neumark,[47] namely,

$$\frac{E_d}{E_d(0)} = 1.00 - 1.81a^*\left(\frac{4\pi e^2}{\kappa k}\right)^{1/2}\left[\frac{N_a}{T}\left(1-\frac{N_a}{N_d}\right)\right]^{1/2} + 0.81a^{*2}\left(\frac{4\pi e^2}{\kappa k}\right)\left[\frac{N_a}{T}\left(1-\frac{N_a}{N_d}\right)\right], \quad (19)$$

where we have assumed that $n \ll N_a$ over the temperature range for which the computer fit of E_d is established most critically, and that the impurity ions are not mobile; i.e., $T_m \to \infty$ in Eq. (13) of Ref. 46. Equation (19) was evaluated at 30 K, a temperature characteristic of the exponential freeze-out region measured. As can be seen from the comparison of the two results, both give reasonably consistent values among the several samples of phosphorus- and arsenic-doped crystals, although the two theories disagree by about 0.5 meV. In all cases, the theory of Neumark gives results closer to the optical activation energy. We are necessarily reluctant to conclude much more than this, since a meaningful test of this problem would require more heavily doped and some heavily compensated samples, which we have not measured.

TABLE VI. Results of fitting the mobility for samples having significant amounts for neutral-impurity scattering using the Erginsoy formula [Eq. (8)].

Sample	N_a (cm^{-3})[a]	A	G	Stand. dev. of fit (10^{-2})	Compensation ratio N_a/N_d[b]
Si: P 1	4.1×10^{12}	1.6	1.00	5.1	0.00044
Si: As 1	6.0×10^{12}	5.9	1.04	3.1	0.00043
Si: As 2	4.3×10^{13}	11.7	0.96	1.1	0.0055
Si: As 3	1.8×10^{13}	6.2	0.74	2.9	0.00024
Si: Sb 1	5.3×10^{12}	1.5	1.11	5.0	0.00072

[a]Values fixed.

[b]N_d and N_a from Table I.

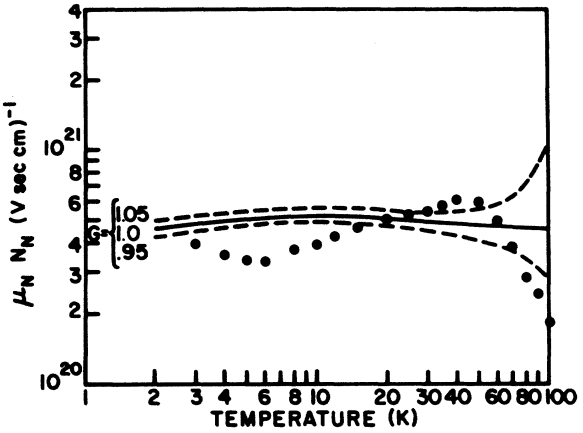

FIG. 11. Temperature dependence of the neutral-impurity scattering mobility for Si: P 1 (normalized to unit density of neutral impurities) shown as solid circles, as calculated from Eq. (17). Solid curve shown for the same procedure, but with the measured mobility replaced by the mobility calculated with Erginsoy's formula, with $A=1.6$ and $G=1.0$. Other values of G are also shown as dashed lines.

In the two cases in which we allowed N_c to vary in fitting Si: P 5 and Si: P 6, the results agree very well with the calculated values. This is not unexpected, but is a satisfying check on our procedure.

B. Mobility Analysis: General

With the exception of neutral-impurity scattering in n-type silicon samples, we have shown that the general procedure outlined by Herring and Vogt[1] can be made to give very accurate results.[48] With a more suitable expression for neutral-impurity scattering, it is expected that the mobility can be calculated to within a few percent between

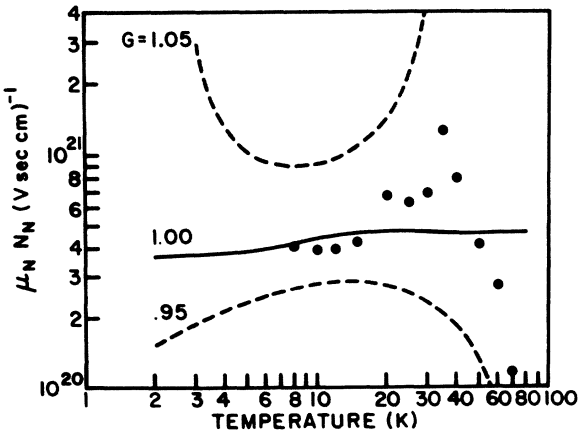

FIG. 12. Same as Fig. 11, for Si: P 5.

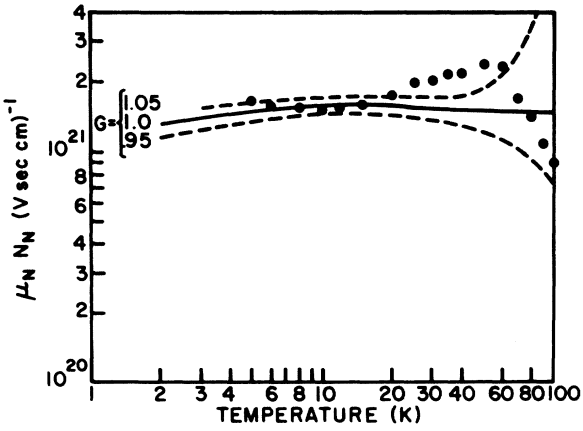

FIG. 13. Same as Fig. 11, for Si: As 1, with calculated curves for $A=5.0$.

20 and 300 K for doping levels less than 10^{17}–10^{18} cm^{-3}. In addition, the Hall factor can also be calculated to about this same level of accuracy. Conversely, the accuracy of the mobility formulation permits us to determine the compensation density if the strength of the ionized-impurity scattering is at least comparable to that produced by neutral impurities. This may be especially useful if uncompensated impurities of two types are present; e.g., $N_{\text{phosphorus}} \sim N_{\text{arsenic}} > N_a$, where the assumption of an equation of the form of Eq. (2) would give ambiguous results. The usefulness of such an alternate approach has been demonstrated by an analysis of impurities in p-type germanium.[10,49]

C. Lattice Scattering

It is of interest to first review the present understanding of this subject, as regards the various

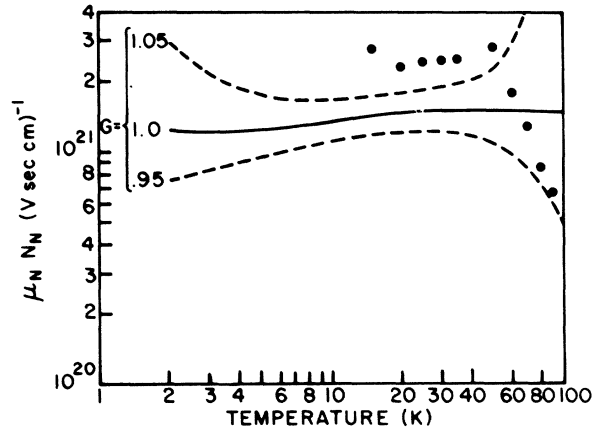

FIG. 14. Same as Fig. 11, for Si: As 2, with calculated curves for $A=5.0$.

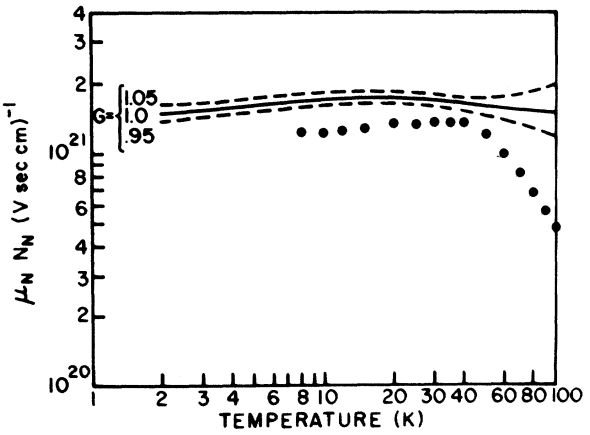

FIG. 15. Same as Fig. 11, for Si: As 3, with calculated curves for $A = 5.0$.

types of intervalley scattering, and the basis upon which several views have been adopted. Information on this subject has been sought in a number of ways; by theory, calculating the allowed intervalley transitions, and in principle, the matrix elements for these transitions; from experimental observations, including optical phenomena such as photoconductivity spectrum, hot electron effects in which intervalley transitions are important in balancing energy gained from the electric field, and, as in our present case, from Ohmic mobility or other transport phenomena.

The allowed transitions for intervalley scattering have recently been agreed upon by the principal authors who have concerned themselves with these calculations. As summarized by Streitwolf,[50] and agreed upon by Lax and Birman,[51] the allowed electron one-phonon selection rules permit LO g-type transitions (at 0.34X), and LA TO f-type transitions (at S on the phonon Brillouin zone face). The characteristic temperatures and energies of these phonons are LO (720 K, 62 meV), LA(560 K, 48 meV), and TO (680 K, 59 meV). It is to be noted that in this respect, no low-energy phonons are possible. An earlier misunderstanding concerning the selection rules had indicated that g-type LA phonons would be allowed, such phonons having energy 21 meV (240 K). Also specifically forbidden are f-type TA phonon transitions. In view of recent work in InSb[52] and Ge,[53,54] however, it is important to keep in mind that although TA f-type and LA g-type transitions are forbidden when considering a one-phonon collision, such restrictions may not apply when other processes are considered. Recent evidence of two-phonon Raman spectral lines in silicon,[55] involving TO and TA phonons, has shown that multiphonon processes are probably very important. The experimental data on Si: P 6 are presently being reanalyzed with two-phonon terms included.[56]

The experimental analysis of intervalley scattering began in 1960 and immediately established two opposing schools of thought. Dumke,[57] analyzing the radiative recombination data of Haynes *et al.*,[58] found contributions from 23-meV phonons (presumed to be g-type at 0.36X) and 46-meV phonons (f-type LA at S) which he assumed were due to intervalley scattering. Evaluating the matrix elements he found g-type scattering to dominate over f type by a factor of 2.5 to 1 at room temperature. The opposite conclusion was simultaneously reached by Long[7] from his analysis of mobility. Long found the higher-temperature phonon, in this case 54 meV (an average of TO, LO, and LA f type), to be dominant in the scattering of electrons, compared to a representative low-temperature phonon of 16 meV. In this case, with Long's coupling constants, f-type scattering (high-temperature phonons) dominates g type at room temperature by a ratio of more than 5 to 1, although the contribution due to acoustic mode intravalley scattering is assumed to be more important in Long's analysis than in Dumke's.[59] This interesting controversy was then taken up by Aubrey *et al.*[59] using piezoresistance and piezo-Hall effect data. Their work supported Long, in that the room-temperature ratio of zero to saturation resistivity could be calculated more accurately with the coupling constants determined by Long.

Asche *et al.*[60] introduced a new twist into this situation on the basis of hot electron experiments. From their data they claim to have shown that g-type scattering is dominant over f type, but assume that g-type scattering can occur with both high- and low-temperature phonons. Thus, using a high-temperature phonon of 62 meV, they fit their data

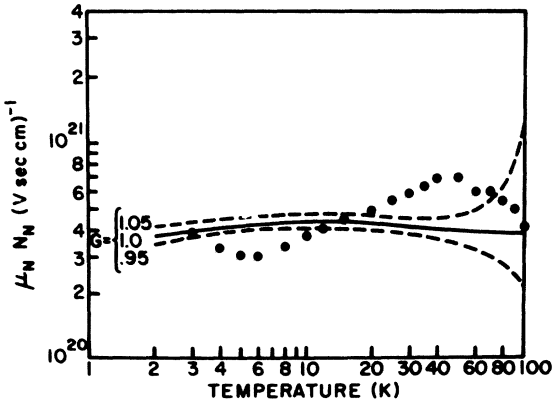

FIG. 16. Same as Fig. 11, for Si: Sb 1, with calculated curves for $A = 1.3$.

TABLE VII. Comparison of calculated activation energies, in the limit of vanishing impurity concentration, for two theories, Penin *et al.* (Ref. 42) and Neumark (Ref. 47).

Sample	E_d from expt. (meV)	Penin *et al.* $E_d(0)$ from Eq. (18) (meV)	Neumark $E_d(0)$ from Eq. (19) (meV)	Optical value of $E_d(0)$ (meV)
Si: P 1	45.64	46.37	45.90	
Si: P 3	45.14	46.43	45.72	
Si: P 4	43.39	46.04	44.95	45.53[a]
Si: P 5	45.38	46.31	45.75	
Si: P 5	45.42	46.32	45.74	
Si: As 1	53.64	54.46	54.01	
Si: As 2	52.54	54.13	53.51	53.73[a]
Si: As 3	52.52	53.71	53.14	
Si: Sb 1	42.59	43.38	42.86	42.73[a]

[a]Value taken from Aggarwal and Ramdas (Ref. 44), but with corrected value of the activation energy of the $3P_{\pm}$ state as calculated by Faulkner (Ref. 45).

with a coupling constant for this phonon of 3.0, and chose the low-temperature phonon coupling constant an order of magnitude smaller. This result is not particularly inconsistent with Long, in that mobility data cannot distinguish an f-type from a g-type process, but is contrary to Dumke, since the high-temperature phonon was found to dominate over the low-temperature one.

A reanalysis of radiative recombination data as measured by Dean *et al.*[61] was made by Folland.[62] His initial result reported in 1968 gave further support to the contention of Long that the higher-temperature intervalley phonon processes were dominant. In this case, Folland found coupling constant values for three modes; 0.44 for a 23-meV phonon, 0.06 for a 46-meV phonon, and 1.5 for a 62-meV phonon. A more refined result, given in 1970 by Folland,[63] gave slightly larger contributions of the low-temperature phonon, now estimated to be 25 meV. Use of these refined coupling constants made it possible to reproduce the mobility data to an accuracy of about 8% between 100 and 300 K. An important consideration in attempting to understand this work is that Folland used selection rules permitting g-type LA phonons (25 meV at $0.40X$). This was based on the earlier results of Lax and Hopfield,[64] and shown to be incorrect by Streitwolf.[50] However, further evidence for a transition involving phonons of about this same energy was reported by Onton[35] in 1969.

The experiments of Onton were based on a prediction by Stocker[65] that intervalley scattering transitions would be evident in the spectral response of extrinsic photoconductivity. Stocker predicted dips in the photocurrent, corresponding to intervalley transitions from states high in the conduction band of one valley to the bottom of the band in another valley. Since the carrier lifetime is much shorter for carriers near the bottom of the band, such transitions should reduce the photocurrent. Onton found such dips corresponding to energy transitions of 27 and 47 meV as analyzed by Stocker's model. The magnitude of the dip was assumed to be indicative of the phonon coupling strength, and roughly equal amounts of g-type (27 meV) and f-type (47 meV) scattering were predicted from the data.

Computations of hot electron effects were made by numerous authors around this same time. In certain cases, the coupling constants of Long were adopted (Jørgensen and Meyer,[66] Kawamura,[67] Jørgensen,[68] Basu and Nag,[69] Holm-Kennedy and Champlin,[70] Glushkov and Markin[71]), while in other cases the coupling constant of Dumke and Onton were used (Costato and Scavo,[72] Costato and Reggiani,[73] Costato, Fontanesi, and Reggiani[74]). As already mentioned, the conclusions of Asche *et al.*[60] and also those of Heinrich and Kriechbaum,[75] did not particularly support either view. We are not prepared to evaluate the validity of any of these calculations, which have at times concluded that g-type scattering was dominant while other workers found f-type scattering more important. Since the experimental measurement of hot electron effects can preferentially heat or cool certain valleys by the choice of electric field orientation and therefore provide information which ought to distinguish g-type and f-type scattering modes, the disagreement in the interpretation of this data is probably due to the extremely difficult nature of the calculations, in which various approximations regarding the carrier distribution function are typically involved. This subject has been reviewed recently by Conwell.[76]

Basu and Nag[77] reviewed the various coupling constant results to see how each predicted the mobility, Hall factor, magnetoresistance coefficient and piezoresistance. Within limits, each model gave a fair fit to the mobility data, but only Long's model was found satisfactory in describing the other measurements. In a following paper, infrared free-carrier absorption data were similarly analyzed by Basu and Nag,[78] and again Long's model gave the closest fit to the data.

Photoresponse measurements made by Nishino and Hamakawa[79] near the indirect gap gave values of the TA- and TO-phonon energies, but no structure due to either LA or LO phonons was observed. The absence of LO modes could support the weakness of g-type scattering, if these data can be considered representative of free-electron intervalley scattering.

Photoconductivity measurements, similar to Onton's have since been reported by two independent groups. The first of these, by Godik and Mirgorodskii,[80] found no evidence of the 27-meV phonon reported by Onton, Dumke, and Folland. They found very slight interaction with TA (f type) and LA (also f type) phonons, but strong interactions with a phonon near 60 meV, LO or TO, which could not be distinguished with their resolution. The second group, Guichar *et al.*,[81] found evidence of the 27-meV phonon. Their measurements were made only in the spectral region beyond 15 μm, so that no measurement of higher-energy modes could be deduced.

The problem of interpreting all of this work in a satisfactory way is clearly difficult, since it would appear that similar measurements in many instances are interpreted with opposite conclusions, and that any argument proposing to include phonons of low temperature is at variance with the calculated selection rules. The concluding remarks of many of these same papers have perhaps prematurely announced the resolution of this problem, so that we will attempt here only to suggest a few ideas which can be further digested into this continuing discussion.

We would like to begin by noting that the experimental samples measured by Onton[35] and by Guichar *et al.*[81] may differ importantly from those used by Godik and Mirgorodskii.[80] These latter authors used moderately doped ($N_d < 1\times 10^{16}$ cm^{-3}), but substantially compensated samples ($N_a > 1\times 10^{14}$ cm^{-3}). While the samples of Onton appear to be in the range of $1-2\times 10^{16}$ cm^{-3}, and those of Guichar *et al.* somewhat higher, in neither case was the compensation density given. Measurements of the oscillatory photoconductivity reported for p-type germanium samples have shown that substantial compensation densities are necessary for the observation of the effect predicted by Stocker.[65] Since the spectrum of dips reported by Godik and Mirgorodskii are much more prominent than either Onton's or those of Guichar *et al.*, it is very likely that the samples of these latter authors have only small amounts of compensating acceptors. In this case, the carrier lifetime may be comparable to or longer than the thermalization time, and the dips predicted by Stocker cannot be expected. On the other hand, these dips can be explained on the basis of a somewhat different model. In the work of Lax[82] on electron-impurity recombination, the probability of electron capture with the emission of an optical phonon is considered. This could take place between conduction states and any of the bound donor states, in principle, although certain selection rules may also apply to this process. As one possible transition, recombination to the $1S(T_1)$ or $1S(E)$ states lying approximately 32 meV below the conduction-band edge could occur via an optical phonon with energy of about 59 meV. Such a process could explain a dip in the photoconductivity at $E_d + 27$ meV. If similar transitions occur directly to the ground state, a dip should be evident at a photon energy of 59 meV in all spectra. Only Guichar *et al.* have clear spectra in that region, and the dip they observe at 59.4 meV is interpreted by them as a TO phonon emitted in the presence of an impurity. A high density of excited states exists from about 12 meV below, up to the bottom of the conduction band, and recombination via TO-phonon emission into these states would be predicted between $E_d + 47$ and $E_d + 59$ meV. Dips may be seen in the region closer to $E_d + 47$ meV, since the excited states are not too closely spaced in this region, but near $E_d + 59$ meV, the effect would be quasicontinuous, and probably not resolvable.

It is natural to ask how the above explanation will vary with compensation, if we are to understand the different results of Onton, Guichar *et al.*, and Godik and Mirgorodskii. Compensation will be important if the process is viewed as taking place with photoexcitation at one impurity center, followed by transport to and recombination at another impurity center. This type of process will require a substantial amount of compensation, since the free carrier must find an ionized donor before substantial energy is lost to competing mechanisms such as acoustic phonon emission. Hence, the conditions are similar to those of Stocker's model. On the other hand, the possibility of this all taking place at a single impurity site will explain why it would be observed in uncompensated samples, and therefore may resolve the problem of understanding the experimental results of Onton and Guichar *et al.* We have reanalyzed the experiments of Onton in Table VIII, on the basis of this alternative explanation. As shown,

TABLE VIII. Analysis of the photoconductivity data taken by Onton (Ref. 35) based on a proposed model in which a photon of energy $h\nu$ is absorbed at an impurity site, leaving the impurity in an excited state, accompanied by the emission of an intervalley phonon of energy $\hbar\omega$. The impurity is assumed to be originally in the $1S$ (A_1) ground state.

Sample	dip A $h\nu$ (meV)	$1S$ (T_1) $\hbar\omega$ (meV)	$1S$ (E) $\hbar\omega$ (meV)	dip B $h\nu$ (meV)	$2P_0$ $\hbar\omega$ (meV)	dip C $h\nu$ (meV)	$2P_\pm$ $\hbar\omega$ (meV)
Sb	69.4	59.9	57.3	89.6	58.3	94.7	58.5
P	71.5	59.9	58.6	92.0	57.9	97.5	58.4
As	80.1	59.0	57.6	100.9	58.6	106.5	59.1

Impurity transition energies

$1S$ (A_1) to:	$1S$ (T_1)	$1S$ (E)	$2P_0$	$2P_\pm$
Sb	9.55[a]	12.14[a]	31.26[b]	36.20[d]
P	11.62[a]	12.95[a]	34.12[c]	39.14[c]
As	21.09[a]	22.50[a]	42.26[b]	47.36[d]

[a]Reference 44, Table IV.
[b]Reference 44, Figs, 3 and 4.
[c]Reference 83, Fig. 1.
[d]Reference 44, Tables II, III, and IV.

by the appropriate choice of excited-state transitions, all the observed dips in photoconductivity can be explained in terms of a phonon of about 58 meV. Our choice of transitions was based on the work of Dean *et al.*[61] in analyzing recombination radiation effects in which an exciton decays in the presence of an impurity, leaving the impurity in an excited state. To summarize, we propose that optical absorption can occur at an impurity site, with the emission of an optical phonon and the simultaneous excitation of the impurity to an excited state.

If the photoconductivity experiments can be reconciled in view of the above comments, a problem yet remains in the analysis of radiative recombination data made by Dumke and Folland. Their analysis has implied intervalley phonons of energy near 23 meV, in contrast to the 27-meV phonons claimed by Onton and Guichar *et al.* If the conduction-band minimum is located at $0.83X$, then the intervalley g-type transitions will occur at $0.34X$. The LA-phonon branch at this point gives an energy of 21 meV. This is substantially less than the energies found by Onton and Guichar *et al.*, but clearly not as far from the value of 23 meV found from the recombination radiation data. Since the LA-phonon dispersion is large in this region, it is possible that recombination radiation is taking place with an LA g-type phonon, but it is unlikely that the precision involved in both experiments can reconcile the 3–4 meV difference in the determination of this phonon energy. It is not entirely clear to us how the recombination radiation analysis should be modified. If the free-electron approximation is considered together with the selection rules, then LA g-type intervalley phonons cannot initiate the recombination process, but perhaps can terminate it without violation.

The remaining problem in all this work is the apparent presence of TA f-type scattering, as found by Long and in this investigation from mobility analysis, and considered important by Holm-Kennedy and Champlin[70] in explaining warm carrier experiments. TA f-type scattering is forbidden by the selection rules, but nevertheless seems to be present in weak amounts. Even these relatively weakly coupled modes are found important for a complete explanation of experimental data; as was shown in Sec. III B. The most amusing statement that could be made to interpret these results is that time reversal symmetry is broken in silicon, since it is this condition which forbids the TA process.[50] More reasonable approaches could be pursued along the lines of two-phonon scattering to resolve this issue. The negligible amounts of LA f-type scattering found in our work, but not expressly forbidden by the selection rules, also remains to be explained.

For comparison and reference, we list in Table IX the calculated values of lattice mobility between 10 and 500 K, using lattice parameters as analyzed from sample Si: P 6 with model III as listed in Table IV. Also shown are the results of Long, as calculated from his parameters. Surprisingly, the mobility values are quite different at low temperatures (18% at 20 K). This may be due to a combination of systematic errors encountered by Long in correcting for the Hall factor, and the use of an isotropic scattering formulation of ionized-impurity scattering based on the Brooks, Herring, and Dingle equations, which overestimates the strength of this type of scattering.

TABLE IX. Calculated lattice mobility using parameters determined from Si: P 6, model III, and listed in Table IV. Also shown for comparison is the result of Long (Ref. 7).

Temperature (K)	Lattice mobility (cm^2/V sec) This result	Long's result[a]
10	5.68×10^5	6.74×10^5
20	2.01×10^5	2.38×10^5
30	1.09×10^5	1.29×10^5
40	7.01×10^4	8.23×10^4
60	3.72×10^4	4.27×10^4
77.5	2.46×10^4	2.77×10^4
100	1.59×10^4	1.75×10^4
130	9.66×10^3	1.03×10^4
160	6.19×10^3	6.46×10^3
200	3.73×10^3	3.81×10^3
250	2.18×10^3	2.26×10^3
300	1.43×10^3	1.47×10^3
350	1.01×10^3	1.06×10^3
400	7.48×10^2	7.82×10^2
500	4.79×10^2	5.07×10^2

[a]Long's results have been calculated for phonon temperatures of 630 and 190 K with coupling constants of 2.0 and 0.15, respectively. A value of $\tau_0 = 4.31\times10^{-9}$ sec was used to give Long's result at 300 K (Ref. 7).

D. Ionized-Impurity Scattering

It is difficult to compare the results of Long and Myers[12] with this present analysis, since they assumed isotropic scattering by ionized impurities, and we have not assumed this to be the case. However, we did find in comparing the theory of Brooks, Herring, and Dingle with that of Samoilovich *et al.* that the former overestimated the strength of ionized-impurity scattering when it was substituted into the prescription given by Herring and Vogt. This is why a larger value of coupling constant for low-temperature intervalley phonon scattering is obtained in model II, Table II, when N_a is fixed rather than varied. Extra intervalley scattering was preferred in this case, since the relative mobility at low temperatures was enhanced, in part compensating for the overestimate of ionized-impurity scattering. The values of w_3 found under these circumstances are nearly identical to the value determined by Long, and in this respect our conclusion that w_3 should be about half the value found by Long can be understood.

A handicap of our work is that more heavily-doped heavily-compensated samples were not measured, so that a test of ionized-impurity scattering could not be made under conditions where this type of scattering dominated the mobility. Keeping in mind the restrictions imposed by remaining in the high-magnetic-field limit, so that Hall-factor corrections are unnecessary, it should be possible to measure somewhat more heavily-doped samples in this same way.

Rode[28] has lately criticized the use of the spherical band approximation for calculating ionized-impurity scattering in germanium and silicon. We believe the failure of his calculation to describe accurately the mobility of electrons at 300 K for "free carrier concentrations" between 10^{16} and 10^{19} cm^{-3} is more complicated than a simple inadequacy of ionized-impurity scattering, whatever the formulation. Redfield and Afromowitz[84] have recently shown that the screening approximations are invalid in the temperature region and impurity concentration region calculated by Rode. More important, we feel, is the questionable association of free-carrier concentration with impurity concentration and the omission of neutral-impurity scattering. For silicon impurities, even assuming a concentration-dependent activation energy, we find that far from all the impurities are ionized at 300 K. For a value of α given by Penin *et al.* and a concentration of phosphorus impurities of 3×10^{17} cm^{-3}, we find 33% are un-ionized at 300 K. With Erginsoy's formula, and $A = 1$, we find the neutral scattering strength is nearly twice that of ionized impurities at 300 K. Extending our calculations to higher concentrations of N_d we can achieve a result exactly opposite to that of Rode, in that the mobility we calculate for zero compensation is less than indicated by experiment. From this it is clear that a very careful treatment, including the possibility of revising the screening formulas, including neutral scattering, and taking into account not only the temperature dependence of the impurity activation energy, but the eventual formation of an impurity band and the need for degenerate statistics, is required to make reliable calculations in this heavily doped region.

To emphasize the above point, we have plotted in Fig. 17 the calculated mobility between donor concentrations of 10^{13} and 10^{18} cm^{-3}, with $A = 1.0$, and the carrier concentration evaluated with an activation energy dependent upon N_I as in Eq. (18). Also shown are the partial mobilities, μ_I and μ_N for ionized and neutral scattering. As can be seen, at the highest concentration of donors, neutral rather than ionized scattering is dominant. Whether this is true in reality is not clear, since at 300 K the partial-wave theory is probably not accurate in calculating the strength of neutral scattering. Nevertheless, the mobility calculated by this assumption is in good agreement with the drift mobility as summarized by Sze and Irvin[19] near concentrations of 10^{18} cm^{-3}. To complete this comparison, we graph the calculated values of resistivity as a function of donor concentration in Fig. 18, along with the curve given by Irvin. Also shown are the values of resistivity for the samples measured in this investigation. Figure 19 shows

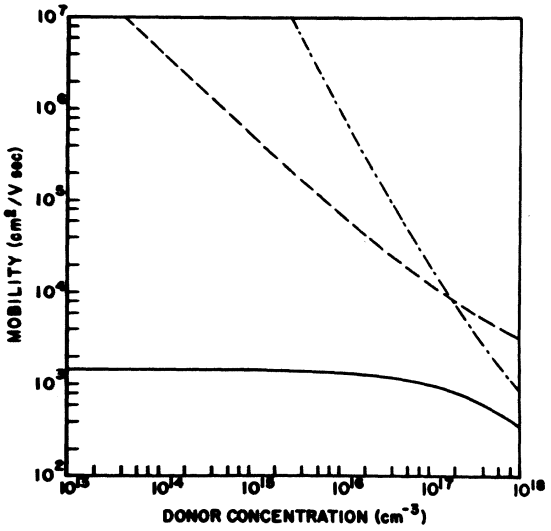

FIG. 17. Electron mobility in n-type silicon as a function of donor concentration at 300 K, as calculated from the equations presented in the text. Also shown are the partial mobilities for ionized (dashed line) and neutral (dash-dot line) impurity scattering.

the Hall factor calculated as a function of donor concentration. The values calculated for this comparison are listed in Table X.

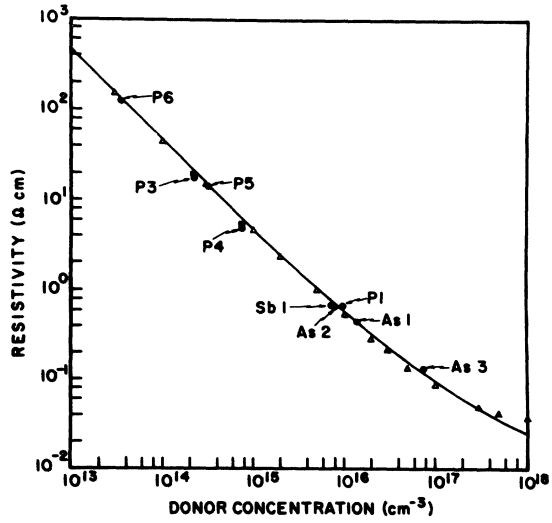

FIG. 18. Calculated resistivity values shown as triangles, compared with the curve of Irvin (Ref. 19) as a function of donor concentration at 300 K. Labeled points show the experimentally determined values from samples measured in this work, circles; while the additional square data points for Si: P 3 and Si: P 4 give the resistivity as corrected by the factor G, given in Table V. Accurate geometry corrections could not be made for the more heavily doped samples studied, since neutral-impurity scattering was important, but not well characterized by theory.

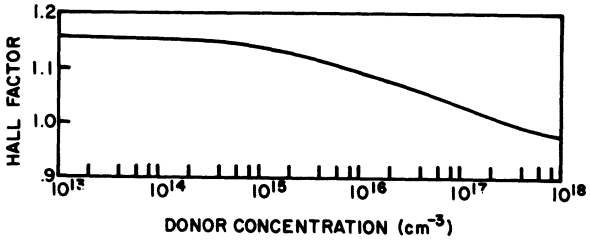

FIG. 19. The Hall factor as a function of donor concentration, as calculated at 300 K.

E. Neutral-Impurity Scattering

The most serious discrepancy between experiment and present theory is evident in the measurements of neutral-impurity scattering. A part of this problem can be resolved in the theory given by Sclar,[9] which included the possibility of bound states in the electron-hydrogenic impurity scattering problem. This was originally suggested by Ansel'm,[85] by noting that hydrogen can have a bound state for two electrons.[86] Sclar's calculation of this effect gives a mobility which varies as $T^{1/2}$ for kT above the binding energy of this two-electron bound state. The data presented in Figs. 11–16 show such a dependence up to 50 K. If values appropriate for silicon are substituted into the expression given by Sclar, the result is not in very good agreement with the data, although the qualitative features are observed. A comparison of Erginsoy's expression and that given by Sclar is shown in Fig. 20. Data from Si: Sb 1 have been included for reference. Examination of the formula given by Sclar shows that more quantitative agreement would be found for a weaker binding energy of the second electron at the impurity center. This conclusion is in conflict with the determination of the binding energy of such centers, as measured by Dean *et al.*[61] and by Gershenzon *et al.*,[87] but in agreement with recent work by Thornton and Honig.[88] We have also plotted the curve for a choice of $\frac{1}{3}E_d^-$, where E_d^- is the binding energy of the second electron at the impurity center, as predicted by the hydrogenic scaling model. Whether fitting the value of E_d^- to the measured mobility data to determine this quantity, as suggested by Sclar, gives a reasonable estimate is open to question, considering the difference in this binding energy determined by other methods. It is also possible that a careful reexamination of the model will give better results, but the conclusion of this must await such calculations. It is encouraging to see that the general increase in neutral mobility up to 50 K can be accounted for by such a model. Much more recent calculations of neutral-impurity scattering at low tem-

TABLE X. Calculated carrier concentration and transport properties as a function of donor density at 300 K.

Donor density (cm^{-3})	Carrier[a] conc. (cm^{-3})	Mobility ($cm^2/V\,sec$)	Resistivity ($\Omega\,cm$)	Hall factor	Partial mobilities ($cm^2/V\,sec$) μ_I[b]	μ_N[c]
1×10^{13}	9.99×10^{12}	1.43×10^{3}	4.38×10^{2}	1.15	3.69×10^{7}	4.79×10^{11}
3×10^{13}	2.99×10^{13}	1.43×10^{3}	1.46×10^{2}	1.15	1.37×10^{7}	6.64×10^{10}
1×10^{14}	9.99×10^{13}	1.43×10^{3}	4.39×10^{1}	1.15	4.49×10^{6}	6.53×10^{9}
3×10^{14}	2.99×10^{14}	1.42×10^{3}	1.47×10^{1}	1.15	1.64×10^{6}	7.45×10^{8}
1×10^{15}	9.94×10^{14}	1.40×10^{3}	4.49×10^{0}	1.14	5.48×10^{5}	7.83×10^{7}
2×10^{15}	1.98×10^{15}	1.38×10^{3}	2.28×10^{0}	1.13	2.95×10^{5}	2.05×10^{7}
5×10^{15}	4.89×10^{15}	1.34×10^{3}	9.54×10^{-1}	1.11	1.32×10^{5}	3.58×10^{6}
1×10^{16}	9.61×10^{15}	1.29×10^{3}	5.05×10^{-1}	1.09	7.29×10^{4}	9.85×10^{5}
2×10^{16}	1.86×10^{16}	1.22×10^{3}	2.75×10^{-1}	1.08	4.12×10^{4}	2.82×10^{5}
3×10^{16}	2.72×10^{16}	1.17×10^{3}	1.97×10^{-1}	1.07	2.99×10^{4}	1.39×10^{5}
5×10^{16}	4.35×10^{16}	1.09×10^{3}	1.32×10^{-1}	1.05	2.03×10^{4}	5.85×10^{4}
1×10^{17}	8.01×10^{16}	9.51×10^{2}	8.21×10^{-2}	1.03	1.24×10^{4}	1.92×10^{4}
3×10^{17}	2.00×10^{17}	6.67×10^{2}	4.69×10^{-2}	1.00	6.14×10^{3}	3.82×10^{3}
5×10^{17}	3.00×10^{17}	5.21×10^{2}	4.00×10^{-2}	0.98	4.59×10^{3}	1.91×10^{3}
1×10^{18}	5.12×10^{17}	3.41×10^{2}	3.58×10^{-2}	0.98	3.18×10^{3}	7.86×10^{2}

[a]Carrier concentration is calculated with a ground-state activation energy according to Eq. (18), with $\alpha=3.6\times10^{-8}$ eV cm. The structures of $1S$ (T_1) and $1S$ (E) states, and the excited states given in Eqs. (2) and (3), are assumed to move towards or even into the conduction band, keeping the same spacing relative to the $1S$ (A_1) ground state. An iterative procedure is used, with E_d chosen intially as 45.4 meV. The value of n determined from this assumption is substituted into Eq. (18) to give a new value of E_d, and the procedure is repeated unitl n changes by less than one part in 10^6.

[b]These values of μ_I are determined from the relaxation times given by Samoliovich *et al.* (Refs. 4–6) given in Eqs. (12)–(15), and are used to calculate the mobility analytically in this case with the usual approximation that the logarithmic term and the terms g_0 and g_1 are taken outside the integral and evaluated at $x=3$.

[c]The neutral-impurity mobility values are calculated from Erginsoy (Ref. 8) with $A=1$. Thus, $\mu_N=3.8\times10^{20}/N_N$ $cm^2/V\,sec$. We chose a value of unity for A so that the data would coincide exactly with the Erginsoy equation, although at 300 K, the approximation used by Erginsoy is no longer valid. An alternate expression, given by Sclar (Ref. 9) using the Born approximation, gives $\mu_N=1.5\times10^{20}/N_N$ $cm^2/V\,sec$ at 300 K. Neither approximation is valid, however, since $|ka|\simeq1$ for silicon at 300 K. The Born approximation, and our experimental data near 100 K, indicate that perhaps even larger neutral-impurity scattering contributions may occur than are indicated above.

peratures have been announced by Blagosklonskaya *et al.*[89] They find a decrease in the mobility at low temperatures, but a temperature-independent mobility at higher temperatures. Such a dependence is not supported by our data. Since both the calculations of Sclar and Blagosklonskaya *et al.* take resonant scattering into account, it is not apparent why different dependencies of temperature exist in their results.

In all samples we have seen a noticeable decrease in the neutral-impurity mobility for temperatures above 50 K, as seen in Figs. 11–16. A natural explanation of this can be found if one considers inelastic collisions between electrons and neutral donors. Such collisions can result in energy transfer to the donor impurity, leaving it in an excited state or even ionized. The minimum carrier energy for which this can occur is given by the splitting of the $1S$ states. Thus, for antimony and phosphorus, about 12 meV is required, while about 21 meV is needed for this transition in arsenic-doped samples. Since the decrease observed begins at about 50 K, for phosphorus and antimony impurities the effect is accounted for with carriers at about $3kT$ or more. For arsenic impurities, the carriers would need to be at $6kT$. Since, however, the mobility is larger in arsenic-doped samples at 50 K, it could be argued that for this impurity a smaller effect will be more noticeable than in the phosphorus- and antimony-doped samples which have lower mobilities at the same temperature. Another way in which the mobility can be lowered at high temperatures is seen by also considering the relative populations of neutral donors in the $1S$ (A_1) state compared to higher-energy $1S$ states (T_1 and E). Since the population of these higher states will be significant above 50 K, it is expected that this will also lower the mo-

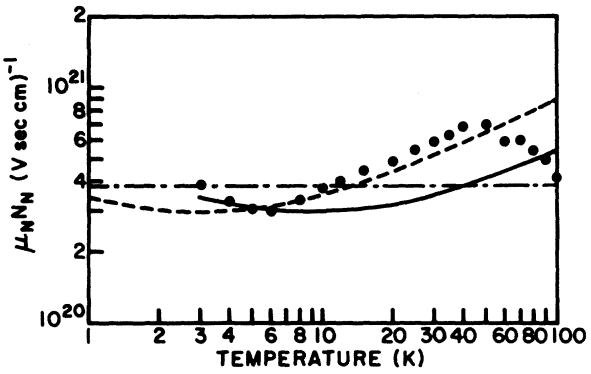

FIG. 20. Comparison of neutral-impurity mobility (for unit density) between Si: Sb 1 (Fig. 16) and the theory of Sclar (Ref. 9), calculated for two choices of the binding energy of the second electron at a donor impurity. The solid line shows Sclar's theory with the binding energy of the second electron scaled from the hydrogen-minus ion according to the effective-mass approximation. The dashed line is calculated for a binding energy of $\frac{1}{3}$ the value calculated from the effective-mass formula. The temperature-independent theory of Erginsoy (Ref. 8) is also shown for comparison as a dash-dot line, with A equal to unity.

bility since the spatial size of the wave function of such states will be larger than for the ground state, and the expected scattering length will be correspondingly greater.

The larger mobility values found for neutral scattering by arsenic impurities in comparison to antimony and phosphorus are not understood. Considering the approximation involved in treating neutral-impurity scattering by the zero-order partial-wave method, one expects the scattering cross section to vary with the square of the scattering length, [10] taken to be the effective-mass Bohr radius in the theory of Erginsoy. Correcting the Bohr radius by the quantum-defect method, one expects the cross section to decrease as the ratio of the effective-mass binding energy to the observed impurity binding energy. This indicates that Erginsoy's result should be multiplied by 1.4, 1.5, and 1.8 to calculate the mobility for antimony, phosphorus, and arsenic, respectively. This is in fair agreement with the averaged computer-fitted values found for A in Table VI, in the case of antimony and phosphorus, but not in good agreement for arsenic-doped samples. We cannot explain this result.

V. SUMMARY AND CONCLUSIONS

Carrier-concentration analysis and mobility analysis have been shown to give excellent agreement in determining the density of compensating acceptor impurities in n-type silicon, when the strength of neutral-impurity scattering was weak to moderate by comparison. In contrast, neutral-impurity scattering has been shown to be poorly described by the present theory, except for the general order-of-magnitude strength in the case of neutral antimony and phosphorus impurities. The density-of-states effective mass, when fit as a parameter in the carrier-concentration analysis of relatively pure samples, has been found to agree well with the values calculated from the established band structure.

A quantitative comparison of several lattice scattering models, currently proposed in the literature, has been made. In particular, we have found that the intervalley scattering contributions can be fitted to a model almost identical to that proposed by Long. This required the inclusion of weakly coupled modes which are forbidden by the selection rules. Other models, based chiefly on data from photoconductivity and radiative recombination data have been examined. Alternative interpretations suggested for some of these data may lead towards a greater concensus on the question of intervalley scattering transitions.

ACKNOWLEDGMENTS

We would like to thank Allen Miller for helpful clarification of the location of the f-type and g-type intervalley phonons. Donald Long kindly supplied us with detailed graphs of his data. We have shared several useful discussions on the selection rules and their implications with Dan Rode, Kai Ling Ngai, and N. O. Folland. The technical assistance of Susan Norton in part of this work is gratefully acknowledged.

---

*Work supported in part by the Air Force Avionics Laboratory.

†Present address: Bell Telephone Laboratories, Allentown, Pa. 18103.

[1] C. Herring and E. Vogt, Phys. Rev. **101**, 944 (1956).

[2] H. Brooks, Phys. Rev. **83**, 879 (1951); in *Advances in Electronics and Electron Physics*, edited by L. Marton (Academic, New York, 1955), Vol. 7, p. 85.

[3] R. B. Dingle, Philos. Mag. **46**, 831 (1955).

[4] A. G. Samoilovich, I. Ya. Korenblit, and I. V. Dakhovskii, Dokl. Akad. Nauk SSSR **139**, 355 (1961) [Sov. Phys.-Dokl. **6**, 606 (1962)].

[5] A. G. Samoilovich, I. Ya. Korenblit, and I. V. Dakhovskii, Fiz. Tverd. Tela **3**, 2939 (1961) [Sov. Phys.-Solid State **3**, 2148 (1962)].

[6] A. G. Samoilovich, I. Ya. Korenblit, I. V. Dakhovskii, and V. D. Iskra, Fiz. Tverd. Tela 3, 3285 (1961) [Sov. Phys.-Solid State **3**, 2385 (1962)].

[7] D. Long, Phys. Rev. **120**, 2024 (1960).

[8] C. Erginsoy, Phys. Rev. **79**, 1013 (1950).

[9] N. Sclar, Phys. Rev. **104**, 1559 (1956).

[10]P. Norton and H. Levinstein, Phys. Rev. B **6**, 470 (1972). The only change in the experimental apparatus was the installation of a new platinum resistance thermometer, a Model 118LX manufactured by Rosemount Engineering.
[11]For a general review of galvanometric measurements, see A. C. Beer, in *Solid State Physics*, edited by F. Seitz and D. Turnbull (Academic, New York, 1963), Suppl. 4.
[12]D. Long and J. Myers, Phys. Rev. **115**, 1107 (1959).
[13]Reference 11, p. 215.
[14]W. Kohn, in Ref. 11, Vol. 5, p. 257.
[15]R. A. Faulkner, Phys. Rev. **184**, 713 (1969).
[16]R. L. Aggarwal, Solid State Commun. **2**, 163 (1964).
[17]J. S. Blakemore, *Semiconductor Statistics* (Pergamon, New York, 1962).
[18]D. Long and J. Myers, Phys. Rev. **115**, 1119 (1959).
[19]J. C. Irvin, Bell Syst. Tech. J. **41**, 387 (1962); S. M. Sze and J. C. Irvin, Solid-State Electron. **11**, 599 (1968).
[20]It is more difficult to accurately measure the length and width between resistivity probes, than to measure the sample thickness. Geometrical errors have been considered in Refs. 10 and 21.
[21]D. Long and J. Myers, Phys. Rev. 120, 39 (1960).
[22]L. J. Neuringer and W. J. Little, in *Proceedings of the International Conference on the Physics of Semiconductors, Exeter, 1962* (The Institute of Physics and the Physical Society, London, 1962), p. 614.
[23]A. G. Kazanskii and O. G. Koshelev, Fiz. Tekh. Poluprovodn. **6**, 953 (1972) [Sov. Phys.-Semicond. **6**, 826 (1972)].
[24]E. Otsuka, K. Murase, and K. Takesawa, in *Proceedings of the Ninth International Conference on the Physics of Semiconductors, Moscow, 1968* (Nauka, Leningrad, 1968), p. 292.
[25]A. Honig and R. Maxwell, in Ref. 24, p. 1117.
[26]F. Ham, Phys. Rev. **100**, 1251 (1955).
[27]L. J. Neuringer and D. Long, Phys. Rev. **135**, A788 (1964)
[28]D. L. Rode, Phys. Status Solidi B **53**, 245 (1972).
[29]The fitting details are given in Ref. 10. Briefly, the parameters are adjusted to minimize the sum of the squares of the difference between the logarithms of experimental and calculated values.
[30]The samples in all cases were approximately 10 mm long, 1 mm thick, and 1.5 mm wide. Three pairs of arms for attaching leads were spaced along the length. Most samples had center to center spacings of the arms of 1.4 mm, and arm widths of 0.7 mm. Sample resistivity was calculated from the voltage drop between one center arm and an adjacent arm. Samples Si:P 5 and Si:P 6 has only two pairs of arms. The two nearest the center, but slightly off set, were used to measure the Hall voltage. One of these and one of the second pair served to measure the voltage drop for computing the resistivity. The arms were spaced by 4.0 mm and were approximately 0.5-mm wide. Thus, the arm-width-to-spacing ratio is much better for these samples. For the other samples, a geometrical factor G was included in the analysis. The parameter G, discussed in Ref. 10, is a constant multiplying the calculated mobility. An adjustment of G can compensate for errors in measuring the sample geometry, as required. See also, Ref. 20.
[31]M. B. Prince, Phys. Rev. **93**, 1204 (1954).
[32]G. W. Ludwig and R. L. Watters, Phys. Rev. **101**, 1699 (1956).
[33]D. C. Cronemeyer, Phys. Rev. **105**, 522 (1957).
[34]J. Messier and J. M. Flores, J. Phys. Chem. Solids **24**, 1539 (1963).
[35]A. Onton, Phys. Rev. Lett. **22**, 288 (1969).
[36]M. Cuevas, Phys. Rev. **164**, 1021 (1967).
[37]D. M. Brown and R. Bray, Phys. Rev. **127**, 1593 (1962).
[38]N. Sclar, Phys. Rev. **104**, 1548 (1956).
[39]P. Norton, T. Braggins, and H. Levinstein, Phys. Rev. Lett. **30**, 488 (1973).
[40]P. Norton and H. Levinstein, Phys. Rev. B **6**, 478 (1972).
[41]G. L. Pearson and J. Bardeen, Phys. Rev. **75**, 865 (1949).
[42]N. A. Penin, B. G. Zhurkin, and B. A. Volkov, Fiz. Tverd. Tela **7**, 3188 (1965) [Sov. Phys.-Solid State **7**, 2580 (1966)].
[43]P. P. Debye and E. M. Conwell, Phys. Rev. **93**, 693 (1954).
[44]R. L. Aggarwal and A. K. Ramdas, Phys. Rev. **140**, A1246 (1965).
[45]The conclusions of Ref. 44 were based on the energy level of the $3P_{\pm}$ state, as calculated by Kohn (Ref. 14), namely 2.90 meV. These have been revised according to the results of Faulkner (Ref. 15) who finds a calculated value of 3.12 meV. Hence, the results of Ref. 44 should be adjusted by 0.22 meV.
[46]G. F. Neumark, Phys. Rev. B **5**, 408 (1972).
[47]These equations include a modificatin of Ref. 46 to include screening by preferential compensation, as provided by Eq. (11) of this paper. We wish to thank Dr. Neumark for sending us this revised treatment prior to publication, and for an interesting discussion of these effects.
[48]E. M. Eagles and D. M. Edwards, Phys. Rev. **138**, A1706 (1965).
[49]P. Norton and H. Levinstein (unpublished data on mercury-doped germanium).
[50]H. W. Streitwolf, Phys. Status Solidi **37**, K47 (1970).
[51]M. Lax and J. L. Birman, Phys. Status Solidi B **49**, K153 (1972).
[52]K. L. Ngai and E. J. Johnson, Phys. Rev. Lett. **29**, 1607 (1972).
[53]P. J. Lin-Chung and K. L. Ngai, Phys. Rev. Lett. **29**, 1610 (1972).
[54]Yu. A. Astrov and A. A. Kastal'skii, Fiz. Tekh. Poluprovodn. **6**, 1773 (1972) [Sov. Phys.-Semicond. **6**, 1528 (1973)].
[55]P. A. Temple and C. E. Hathaway, Phys. Rev. B **7**, 3685 (1973).
[56]The two-phonon analysis is being conducted in collaboration with Kai Ling Ngai at the Naval Research Laboratory, who suggested this process to one of us (P.N.) as a possible explanation for our experimental evidence of TA phonon scattering.
[57]W. P. Dumke, Phys. Rev. **118**, 938 (1960).
[58]J. R. Haynes, M. Lax, and W. F. Flood, J. Phys. Chem. Solids **8**, 392 (1959).
[59]J. E. Aubrey, W. Gubler, T. Henningsen, and S. H. Koenig, Phys. Rev. **130**, 1667 (1963).
[60]M. Asche, B. L. Boichenko, W. M. Bondar, and O. G. Sarbej, in Ref. 24, p. 793.
[61]P. J. Dean, J. R. Haynes, and W. F. Flood, Phys. Rev. **161**, 711 (1967).
[62]N. O. Folland, Phys. Lett. A **27**, 708 (1968).
[63]N. O. Folland, Phys. Rev. B **1**, 1648 (1970).
[64]M. Lax and J. J. Hopfield, Phys. Rev. **124**, 115 (1961).
[65]H. J. Stocker, Solid State Commun. **6**, 125 (1968).
[66]M. H. Jørgensen and N. I. Meyer, Solid State Commun. **3**, 311 (1965).
[67]N. Kawamura, J. Phys. Chem. Solids **27**, 919 (1966).
[68]M. H. Jørgensen, Phys. Rev. **156**, 834 (1967).
[69]P. K. Basu and B. R. Nag, Phys. Rev. B **1**, 627 (1970).
[70]J. W. Holm-Kennedy and K. S. Champlin, J. Appl. Phys. **43**, 1878 (1972); J. Appl. Phys. **43**, 1889 (1972).
[71]M. V. Glushkov and A. I. Markin, Fiz. Tverd. Tela **14**, 3525 (1972) [Sov. Phys.-Solid State **14**, 2967 (1973)].
[72]M. Costato and S. Scavo, Nuovo Cimento B **52**, 236 (1967); Nuovo Cimento B **54**, 169 (1968).
[73]M. Costato and L. Reggiani, Nuovo Cimento B **58**, 489 (1968); Phys. Status Solidi **38**, 665 (1970); Phys. Rev. B **3**, 1501 (1971).
[74]M. Costato, S. Fontanesi, and L. Reggiani, Nuovo Cimento Lett. **1**, 946 (1969); J. Phys. Chem. Solids **34**, 547 (1973).

[75]H. Heinrich and M. Kriechbaum, J. Phys. Chem. Solids **31**, 927 (1970).
[76]E. M. Conwell, in Ref. 11, Suppl. 9.
[77]P. K. Basu and B. R. Nag, Phys. Rev. B **5**, 1633 (1972).
[78]P. K. Basu and B. R. Nag, Phys. Status Solidi B **53**, K61 (1972).
[79]T. Nishino and Y. Hamakawa, Phys. Status Solidi B **50**, 345 (1972).
[80]E. E. Godik and V. I. Mirgorodskii, Fiz. Tekh. Poluprovodn. **6**, 826 (1972) [Sov. Phys.-Semicond. **6**, 715 (1972)].
[81]G. M. Guichar, F. Proix, C. Sebenne, and M. Balkanski, Phys. Rev. B **5**, 3013 (1972).
[82]M. Lax, Phys. Rev. **119**, 1502 (1960).
[83]R. L. Aggarwal and A. K. Ramdas, Phys. Rev. **137**, A602 (1965).
[84]D. Redfield and M. A. Afromowitz, Philos. Mag. **19**, 831 (1969).
[85]A. I. Ansel'm, Zh. Eksp. Teor. Fiz. **24**, 85 (1953).
[86]S. Chandrasekhar, Rev. Mod. Phys. **16**, 301 (1944).
[87]E. M. Gershenzon, G. N. Gol'tsman, and A. P. Mel'nikov, Zh. Eksp. Teor. Fiz. Pis'ma Red. **14**, 281 (1971) [JETP Lett. **14**, 185 (1971)].
[88]D. Thornton and A. Honig (private communication).
[89]L. E. Blagosklonskaya, E. M. Gershenzon, Yu. P. Ladyzhinskii, and A. P. Popova, Fiz. Tverd. Tela **11**, 2967 (1969) [Sov. Phys.-Solid State **11**, 2402 (1970)].